Utilizing Drones to Assess the Body Condition of Tamanend's Bottlenose Dolphins in the Charleston Estuarine System

Colin M. Perkins-Taylor,[1,2] Wayne E. McFee,[3] Daniel J. McGlinn,[4] Thomas W. Greig,[3] and Norman S. Levine[5]

[1]*Consolidated Safety Services (CSS) Inc., under contract to National Oceanic and Atmospheric Administration (NOAA), National Ocean Service (NOS), National Centers for Coastal Ocean Science, Charleston (NCCOS), SC 29412, USA*
E-mail: colin.perkins-taylor@noaa.gov

[2]*College of Charleston, Graduate Program in Marine Biology, Charleston, SC 29424, USA*

[3]*National Oceanic and Atmospheric Administration (NOAA), National Ocean Service (NOS), National Centers for Coastal Ocean Science (NCCOS), Charleston, SC 29412, USA*

[4]*College of Charleston, Department of Biology, Charleston, SC 29424, USA*

[5]*College of Charleston, Department of Geology and Environmental Geosciences, Charleston, SC 29424, USA*

Abstract

Body condition is a measure of an animal's energy reserves relative to its body structure that provides important information about individual- and population-level health. Monitoring the body condition of free-ranging cetaceans has historically been difficult, but in recent years, the unmanned aerial system (UAS, or "drone") has facilitated noninvasive ways of estimating the cetacean body condition. The Charleston Estuarine System (CES) includes the estuarine and coastal ecosystems surrounding Charleston, South Carolina, and is utilized by Tamanend's bottlenose dolphins (*Tursiops erebennus*) throughout the year. The main goals of this study were (1) to test if UASs are suitable for monitoring body condition of dolphins in an estuarine environment, and (2) to determine if site, season, and age class influence the body condition of dolphins in the CES. Land-based UAS surveys were conducted at four sites throughout the CES between September 2022 and May 2023. The body condition of each dolphin was evaluated using images of the individual positioned flat with a straight body at the surface, and a linear

mixed effects model was constructed to determine which effects were associated with significant differences in dolphin body condition. After filtering images for quality, 428 images of 174 unique dolphins were included in the final analysis, with repeated body condition estimates of 24 dolphins from multiple seasons. Both season and age class were significant predictors of dolphin body condition, but site was not. In addition, individual dolphins were catalogued in a Drone Dolphin ID database, which allowed some dolphins' unique body condition changes to be tracked over time. These findings provide an important baseline for dolphin body condition in the CES that can be built upon in future studies to better understand how body condition changes in response to environmental and anthropogenic stressors or for different age classes.

Keywords: body condition, energy reserves, unmanned aerial system (UAS), drones, aerial photogrammetry, health monitoring, Tamanend's bottlenose dolphin, *Tursiops erebennus*

Introduction

Assessing the body condition of animals provides crucial information about the life history and health status of individuals and populations. For cetaceans, body condition is considered to be the amount of energy reserves that the animal has relative to its structural size (Peig & Green, 2009). Body condition is particularly important for the survival and reproductive success of cetaceans, both of which are typically greater when the individual is in better body condition and thus has more energy reserves (Miller et al., 2012). For instance, North Atlantic right whales (*Eubalaena glacialis*) in poor body condition experience reduced growth rates, survival, and reproductive success, and poor body condition is a key indicator of declining health for southern resident killer whales (*Orcinus orca*) (Fearnbach et al., 2018; Christiansen et al., 2020). Additionally, the body condition of female cetaceans is a strong indicator of how likely they are

to successfully reproduce and raise their young (Kershaw et al., 2021). Female harbor porpoises (*Phocoena phocoena*) in poor body condition are less likely to conceive (IJsseldijk et al., 2021), and pregnant female common minke whales (*Balaenoptera acutorostrata*) in poor body condition decrease energy investment into their fetuses (Christiansen et al., 2014). Collectively, these studies demonstrate the negative impacts that poor body condition can have on the long-term survival and viability of cetacean populations.

Despite the valuable information that body condition provides about individual and population health, monitoring the body condition of free-ranging cetaceans has historically been challenging because most species are highly difficult or impossible to capture depending on size, spend the majority of their time submerged underwater, and present limited opportunities for visual examination when they surface briefly to breathe (Nowacek et al., 2016). In the past decade, unmanned aerial systems (UASs), also known as drones, have emerged as a popular and powerful tool that have revolutionized how free-ranging cetaceans are studied in the wild (Durban et al., 2015). Compared to traditional cetacean health assessment methods such as boat-based surveys, manned aircraft surveys, and live capture-release health assessments, UASs are relatively inexpensive, easy to transport and use in the field, can access remote areas that otherwise are difficult to monitor, and are minimally stressful to the animal due to their noninvasive nature (Hodgson et al., 2016; Atkinson et al., 2021). Furthermore, UASs provide greater aerial observation time of free-ranging cetaceans that have enabled researchers to view these animals from a novel perspective and collect frequent full body images and videos of them, thus advancing the field by allowing new research questions to be addressed.

One of the most common ways that UASs have been employed to study free-ranging cetaceans is using aerial photogrammetry to indirectly estimate their body condition. To date,

cetacean body condition studies utilizing UASs have primarily focused on larger baleen whale species at their foraging and breeding grounds because they undergo drastic body condition changes over a relatively short period of time due to long distance migration (Christiansen et al., 2016, 2018, 2021; Lemos et al., 2020; Bierlich et al., 2022; Torres et al., 2022). In more recent years, UAS body condition and aerial photogrammetry studies focused on odontocetes have become more common. For example, UAS body condition and photogrammetry studies have been conducted on the two largest members of the Delphinidae family, killer whales and short-finned pilot whales (*Globicephala macrorhynchus*), as well as smaller species like Australian snubfin dolphins (*Orcaella heinsohni*), Australian humpback dolphins (*Sousa sahulensis*), Indo-Pacific humpback dolphins (*Sousa chinensis*), franciscanas (*Pontoporia blainvillei*), Guiana dolphins (*Sotalia guianensis*), and beluga whales (*Delphinapterus leucas*) (Fearnbach et al., 2020; Durban et al., 2021; Stewart et al., 2021; Arranz et al., 2022; Christie et al., 2022; de Oliveira et al., 2023; Serres et al., 2024; Sherrill et al., 2024). While the focus of most studies are on body condition, UASs have also been used to identify pregnant common bottlenose dolphins (*Tursiops truncatus*) based on body width-length ratios (Cheney et al., 2022).

Evaluating a cetacean's body condition typically involves measuring the animal's total length and body widths at various points along the body axis from UAS-captured images, calculating a ratio between those measurements, and then comparing variation in the ratio and/or measurements between individuals (Christiansen et al., 2016; Burnett et al., 2018). However, the specific body condition metric used across most of these UAS studies (Christiansen et al., 2020; Fearnbach et al., 2020; Durban et al., 2021), particularly for small cetacean species (e.g., de Oliveira et al., 2023; Serres et al., 2024; Sherill et al., 2024), has been inconsistent and makes comparisons between species and studies difficult.

The Body Area Index (BAI) is a two-dimensional standardized body condition metric that was originally developed to estimate whale body condition from UAS aerial imagery (Burnett et al., 2018). BAI has numerous advantages compared to other one- and three-dimensional body condition metrics and has been used to study the body condition of numerous baleen whale species, including blue whales (*Balaenoptera musculus*), gray whales (*Eschrichtius robustus*), humpback whales (*Megaptera novaeangliae*), and Antarctic minke whales (*Balaenoptera bonaerensis*) (Burnett et al., 2018; Lemos et al., 2020; Bierlich et al., 2021b, 2022; Torres et al., 2022). However, BAI has never been used to assess the body condition of an odontocete species. Previous studies have suggested that differences in body condition may be population-specific even within the same or closely related species (Christiansen et al., 2020; Serres et al., 2024), indicating that fundamental research questions such as how body condition varies seasonally need to be investigated independently for any cetacean population of interest. Since it is standardized, BAI may be an optimal body condition metric to address these research questions, although it needs to be tested on a small cetacean species.

The Charleston Estuarine System (CES) is comprised of all the estuarine and coastal waters near Charleston, South Carolina, and is inhabited by Tamanend's bottlenose dolphins (*Tursiops erebennus*) throughout the entire year (Zolman, 2002; Speakman et al., 2006, 2010; Costa et al., 2022). However, different Tamanend's bottlenose dolphin populations utilize the CES seasonally, including year-round residents, seasonal residents, and transients (Zolman et al., 2002; Speakman et al., 2010). The resident dolphin population, known as the Charleston Estuarine System Stock (CESS; Waring et al., 2009), is estimated to be between 265 and 319 individuals (Speakman et al., 2010; Bouchillon et al., 2020). Seasonal resident and transient dolphins typically migrate into the CES during spring and summer before leaving the area during

fall and winter, which causes significant seasonal and annual variation in dolphin abundance in the CES (Zolman, 2002; Speakman et al., 2010). However, it is worth noting that seasonal resident and transient dolphins are primarily associated with coastal areas when they are in the CES whereas resident CESS dolphins are more commonly found in the inshore estuarine waters (Speakman et al., 2006; Laska et al., 2011; Bouchillon et al., 2020). While CESS dolphins move between areas of the CES using coastal waters, they are distinct from the seasonal resident and transient animals that live in or migrate through coastal waters (Speakman et al., 2006), although these populations do interact with one another in nearshore coastal waters, particularly during summer (Laska et al., 2011). Overall, this means that the CES may be inhabited by a composite of dolphins from these distinct populations at any given time.

Bottlenose dolphin distribution patterns have previously been shown to vary based on numerous factors, including sex, season, and age, as well as across multi-year time periods (Owen et al., 2002; McHugh et al., 2011; Hartel et al., 2014; Sprogis et al., 2016). For CESS dolphins specifically, their distribution has been shown to differ based on sex and season, with males typically being more widely dispersed than females (Bouchillon et al., 2020). Interestingly, approximately 42% of dolphins exhibit high site fidelity to localized areas within the CES (Speakman et al., 2006). Within these localized areas, differences in habitat condition and level of anthropogenic disturbance may drive variation in CESS dolphin body condition. CESS dolphins range from Price Inlet to the North Edisto River, and local habitat conditions are highly variable across this large geographic range (Waring et al., 2009). For instance, dolphins in the Charleston Harbor are most likely exposed to various anthropogenic stressors such as noise pollution, rope entanglements, boat strikes, and other human interactions since it is one of the busiest shipping ports on the Atlantic coast (McFee & Lipscomb, 2009; Transue et al., 2023). By

comparison, the Folly River nursery corridor behind the coastal barrier islands of the CES is relatively undisturbed, surrounded by salt marsh, and has little to no human development (McFee et al., 2014). Given the vast differences between these locations, it seems plausible that CESS dolphins exhibiting high site fidelity to these areas may experience distinct local habitat conditions that ultimately influence their body condition and health.

The primary goals of this study were (1) to test the effectiveness of using UASs to estimate the body condition of a small cetacean in an estuarine environment using BAI as the body condition metric, and (2) to assess if various factors, including site, season, and age class, influence CESS dolphin body condition. Since body condition is an important indicator of cetacean health, the findings from this study will provide valuable insight into how dolphin health varies in the CES over time. UASs have previously been used in the CES to monitor the distribution of dolphins in low salinity habitats (Principe et al., 2023), but no health assessment or individual dolphin monitoring has been attempted in this region using UASs. Furthermore, live capture-release dolphin health assessments have occurred infrequently in the CES over the past couple of decades (Fair et al., 2006). Therefore, estimating dolphin body condition with UASs may provide a viable alternative approach to monitoring dolphin health that could lead to more consistent and less invasive health assessment efforts of free-ranging dolphins in the CES.

Methods

Study Area

This study was conducted in estuarine waters at four sites throughout the CES, which includes the Charleston Harbor and all of the surrounding rivers and waterways (32.7694° N, -79.8953° W; Figure 1). The four study sites where surveys were conducted include (1) the Folly River, a

nursery area for CESS dolphin mom–calf pairs behind the CES barrier islands along Folly Beach (McFee et al., 2014); (2) the Stono River Estuary, a relatively undisturbed waterway with small branching creeks that is surrounded by salt marsh and may have some contamination from an old shipyard upriver and a nearby airport (Speakman et al., 2006); (3) James Island Creek, a small creek branching off of the Charleston Harbor on James Island that has poor water quality and is suspected to have high pathogen prevalence (Varlik, 2019); and (4) the waters off the eastern shore of Drum Island, which is a deep water confluence area where the Charleston Harbor collides with the Cooper and Wando Rivers (Figure 1). Additionally, the Drum Island confluence site is a CESS dolphin core use area that is subject to frequent container ship traffic and may be exposed to pollutants and other toxins released from Superfund Sites along the Cooper River (Bouchillon et al., 2020; U.S. Environmental Protection Agency [EPA], 2021). Water clarity throughout the CES is poor because of strong semi-diurnal tidal currents, high productivity, and soft substrate (Van Dolah et al., 1990).

UAS Survey Methodology

Land-based UAS surveys to assess dolphin body condition were conducted monthly at each of the four sites between September 2022 and May 2023. This time period covered fall (September to November), winter (December to February), and spring (March to May) to maximize the likelihood of encountering only CESS dolphins for body condition assessment. Surveys were not conducted during summer (June to August) because this is when the greatest number of seasonal resident and transient bottlenose dolphins are present in the CES, and these animals may experience different body condition trends than resident CESS dolphins based on their distinct life histories (Speakman et al., 2010). Each of the sites were surveyed four times per month

throughout the study period, meaning that a total of 16 UAS surveys were conducted per month. The only exception to this was in September 2022 when Hurricane Ian prevented safe UAS flights at the end of the month. As a result, the five remaining September surveys were conducted in October 2022 instead. A random sequence generator (www.random.org/ sequences) was used to determine the order that the sites were surveyed each month to minimize sampling bias. Two surveys were sometimes performed on the same day, but the same site was never sampled twice on the same day. The UAS used for this study was a DJI Air 2S (SZ DJI Technology Co., LTD, Nanshan, Shenzhen, China), a relatively small and inexpensive consumer quadcopter (183 × 253 × 77 mm). It also includes a stock camera with a 20-megapixel one inch sensor (13.05 × 8.82 mm), 22 mm focal length, and an 8.38 mm f/2.8 fixed aperture lens. All videos were recorded in 5.4K resolution (5,472 × 3,078 image resolution) at 30 frames per second, which made the pixel size approximately 0.0024 mm. During all flights, the UAS was remotely controlled using the DJI Fly app on an iPhone 13 (Apple Inc., Los Altos, CA, USA) connected to the remote controller. Flights typically lasted between 15 and 22 min per battery. All UAS flights were piloted by a U.S. Federal Aviation Administration (FAA) licensed remote pilot (FAA Part 107 operator) in compliance with FAA airspace regulations. Furthermore, all flights over dolphins were conducted under the National Marine Fisheries Service (NMFS) Southeast Region Permit #21938-03.

The surveys conducted during this study were nonsystematic by design because the UAS's battery life was limited. Therefore, maximizing flight time over as many dolphins as possible while they were in range of the UAS was prioritized to increase the amount of potential footage that could be used for body condition assessment. At the start of each survey, the water was visually scanned from land for 5 to 10 min to determine if any dolphins were present. If

dolphins were identified during the initial observation period, the UAS was launched to an altitude between 15 to 30 m above the water to pursue dolphins and record videos of them during surfacing events. If no dolphins were identified during the initial observation period, the UAS was flown over the water to scan for dolphins between 25 to 60 m above sea level with the camera gimbal angled between 30° to 40° during flight. Regardless of the situation, the launch height of the UAS (i.e., the distance from the water's surface to the camera lens) was measured prior to launching the UAS from its land-based home point to account for the altitude on the onboard barometer being set at zero at its launch point. By adding the launch height of the UAS to the recorded barometer altitude, this accounted for any bias introduced by the UAS's launch point altitude being set at zero on the barometer (Bierlich et al., 2021a). For this reason, the UAS was often launched from a dock or platform just above the surface of the water to minimize the launch height as much as possible. In addition, environmental data were also recorded at the start of each flight, including air temperature, wind speed, wind direction, tidal state, cloud cover percentage, Beaufort Sea State (BSS), visibility, and time. All UAS flights were conducted under safe environmental conditions—for example, no precipitation, light wind speeds (< 15 kts), low BSS (≤ 3), and good visibility (≥ 9.5 km).

During each survey, a new dolphin sighting began once a dolphin or group of dolphins were observed in the UAS live video feed. To initiate a sighting, the pilot remotely triggered the UAS to begin recording video. A group was considered to be all dolphins in close proximity to one another (< 100 m) that were exhibiting similar behavior and moving in the same direction (Wells et al., 1987). After starting the sighting, the UAS was positioned directly above the dolphins at an altitude between 20 to 30 m and the camera was angled vertically down at 90° in the nadir position using the gimbal. Efforts were made to record the dolphins in the center of the

camera frame throughout the entire sighting to minimize lens distortion effects (Burnett et al., 2018), but this was not always possible since dolphin movements are quick and less predictable than larger cetacean species like gray and humpback whales (Christiansen et al., 2018; Lemos et al., 2020). If the dolphins' behavior was predictable and they exhibited no responses to the UAS, the UAS was gradually lowered from its initial hovering altitude down to approximately 9.2 m (~30 feet), the lowest altitude permitted for body condition imagery per permit regulations. These low altitude descents captured high resolution imagery that more clearly outline the focal animal's body shape in the water, which improved the accuracy of BAI for body condition assessment. Ideal body condition footage during a sighting included dolphins surfacing in a flat position with a straight body axis. For some sightings, multiple UAS flights were required to obtain adequate dolphin body condition footage of the individual or group. However, some sightings obtained no adequate body condition footage because the dolphins were never flat at the surface, traveled out of the UAS range, or were briefly sighted and then disappeared. Environmental factors such as poor water clarity and sun glare also prevented obtaining adequate body condition footage during some surveys, although this was minimized as much as possible. At the end of any flight where footage of dolphins was taken, a calibration object of known length (1.0 or 1.52 m) was recorded in video between 9.2 and 20 m of UAS altitude to correct for barometric altimeter errors during post-processing (Burnett et al., 2018; Lemos et al., 2020).

Since the study was land-based, dorsal fin photos for photo-ID were only taken opportunistically when dolphins traveled close to shore using a Canon EOS 1DX (Canon, Ōita, Japan) equipped with a 100-400 mm zoom lens. For each dolphin sighting, the total number of dolphins observed and the number of mom–calf pairs present were recorded. At the end of each survey, the number of dolphin sightings and the total number of dolphins observed during the

survey were also recorded. Any potential dolphin behavioral responses to the UAS were also noted for each sighting.

UAS Data Processing

All UAS videos were reviewed during post-processing using *VLC Media Player*, Version 3.0.18 (VideoLAN, Paris, France). During each UAS flight, the "Video Subtitles" option was turned on in the DJI Fly app, which allowed information such as latitude, longitude, and altitude to be viewed in real time for each video during post-processing. For each dolphin sighting, the initial coordinates where the dolphin or group of dolphins were observed in the video were recorded. While reviewing the footage from each flight, still images of dolphins were extracted from the UAS video any time an individual surfaced with their entire body visible in a flat orientation using the "Take Snapshot" function in the *VLC Media Player* software. The UAS altitude for each image was determined by adding the UAS launch height to the UAS altitude taken from the video. To ensure that the final analysis only included high-quality images where dolphins were positioned relatively flat with a straight body axis such that their BAI could be accurately calculated, each image was graded following the photo selection criteria developed by Christiansen et al. (2018). In short, seven attributes were evaluated separately for each image: (1) camera focus, (2) body straightness (horizontally), (3) degree of body roll, (4) degree of body arch, (5) body pitch (vertically), (6) body length measurability, and (7) body width measurability (Christiansen et al., 2018). Each attribute was graded as a 1 (good quality), 2 (medium quality), or 3 (poor quality), and the total image score was calculated as the sum of the grades for each attribute. Any image that received a score of 3 in any attribute or had a total image score ≥ 11 (i.e., four or more image attributes received a score of 2, meaning that more than half of the

attributes were of medium quality) was removed from the final dataset used for statistical analyses. For each flight where dolphin images were taken, two to four still images of the calibration object at altitudes similar to the dolphin images were also extracted from the UAS video following the same procedures.

Individual dolphins were identified from UAS videos based on unique skin pigmentation patterns, scars, tooth rakes, and skin lesions (Cheney et al., 2022). These distinct markings enabled identification of some dolphin individuals during multiple surveys across seasons and sites throughout the study period (Figure 2). All dolphins that had images taken were given a unique Dolphin ID number that was assigned to them for the study's duration. A Dolphin ID database based on UAS images was developed during the study (hereafter known as the Drone Dolphin ID database). The best image(s) of each individual dolphin displaying their distinct markings and features were added to the Drone Dolphin ID database with their corresponding Dolphin ID. For each survey, dolphin images were compared to individuals in the Drone Dolphin ID database to confirm IDs. If the image(s) did not match any known individuals, the dolphin was assigned a new Dolphin ID and added to the database. When dorsal fin photos were taken opportunistically from land, the highest quality photograph for each dolphin was selected for photo-identification (photo-ID) and added to the Drone Dolphin ID database for the corresponding individual. Dorsal fin photographs were evaluated by researchers from the National Marine Mammal Foundation (NMMF) in Charleston, South Carolina, and matched to individuals from the Charleston bottlenose dolphin dorsal fin catalogue in *Finbase* (Adams et al., 2006; Speakman et al., 2010). When matches were successfully made to the Charleston catalogue, any known information about the animal was added to the Drone Dolphin ID database such as sex, age, sighting history, body length, and areas frequented in the CES.

Each dolphin individual was assigned into a demographic unit based on sex (male, female, or unknown), age class (adult or calf), and if they were a presumed mother (yes or no). Assignments for each demographic unit were determined using UAS videos and known information about each dolphin from long-term photo-ID sighting histories and/or health assessments (Zolman, 2002; Fair et al., 2006; Speakman et al., 2010). All dolphins were assumed to be adults except when a small dolphin (sometimes with fetal folds) was observed consistently swimming tightly against another larger dolphin's mid-lateral flank in echelon position (Noren, 2008). In these cases, the small dolphin was assumed to be a calf, and the larger dolphin was assumed to be the lactating mother. During some surveys, the genitalia of socializing dolphins were visible in UAS video, allowing their sex to be determined. If the sex of a dolphin could not be determined using any of these methods, its sex was assigned as unknown. All of this information was collectively stored in the Drone Dolphin ID database and updated throughout the study period as more information became available during subsequent UAS surveys.

Photogrammetry and Body Condition Assessment

The total length (TL), measured from the tip of the rostrum to the notch between the tail flukes, and body widths at 10% intervals along the TL of the body were measured for each dolphin image using *MorphoMetriX*, Version 1.0, open-source photogrammetry software (Torres & Bierlich, 2020). For calibration object images, the TL of the known-length calibration object (PL) was measured using the same software. All of these measurements were in pixels. The *CollatriX*, Version 1.0, open-source software altitude calibration function was used to correct for altitude errors from each UAS flight based on measurements of the known-length calibration object (Burnett et al., 2018; Bird & Bierlich, 2020). The *MorphoMetriX* outputs for dolphin

329 images from each flight were collated using *CollatriX*, with the output from the altitude
330 calibration function being used as the safety (Bird & Bierlich, 2020). BAI was calculated using
331 the whale body condition function in CollatriX (Bird & Bierlich, 2020), which estimates surface
332 area (SA) of the animal by fitting a parabola through each perpendicular width point on both
333 sides of the animal and calculating the area under each parabola (Figure 3; Burnett et al., 2018).

334 To compare the body condition of dolphins in the CES between sites, seasons, and age
335 classes, BAI was calculated for each dolphin image that satisfied the photo selection criteria.
336 BAI was developed based on the body mass index (BMI) formula that is used to estimate human
337 health (BMI = mass [kg]/height [m^2]; Gallagher et al., 1996), but it uses the SA of the animal
338 instead of body mass across a defined Head-Tail Range (Burnett et al., 2018; Bierlich et al.,
339 2021b). BAI is calculated using the following equation:

340 $$BAI = \frac{SA}{(Head - Tail_{Range} \times TL)^2} \times 100$$

341 The optimal Head-Tail Range for estimating the animal's BAI should only include areas of the
342 body that vary in size in response to the individual's energy stores. Cetaceans do not store energy
343 reserves in their head, tail flukes, or pectoral fins (Brodie, 1975; Christiansen et al., 2016), so
344 previous BAI studies of large whales have altered the Head-Tail Range based on species and age
345 class (Bierlich et al., 2021b, 2022; Torres et al., 2022). For this study, the Head-Tail Range used
346 for adults and calves was between 20 to 80% of the TL (Figure 3).

347 BAI was chosen as the comparative body condition metric for a variety of reasons. First,
348 the main benefit of BAI is that it is unitless and scale invariant, which means that body condition
349 can be directly compared within and between individuals over time regardless of differences in
350 body length (Burnett et al., 2018). Another advantage of BAI is that it has high precision and low
351 uncertainty compared to other one- and three-dimensional body condition metrics (Bierlich et al.,

2021b), making it an optimal metric for pilot studies evaluating the body condition of a cetacean population using the UAS. In addition, BAI can still reliably estimate animal body condition from UAS images with uncertain altitude by calculating BAI from raw pixel count values (hereafter known as "pixel images") instead of scaled metric values (hereafter known as "scaled images") (Burnett et al., 2018; Lemos et al., 2020; Torres et al., 2022). This is because BAI is independent of scaling errors that may occur between pixels and metric units during photogrammetry, so calculating BAI with raw pixel values and scaled metric values produces the same BAI value (Burnett et al., 2018; Lemos et al., 2020). During this study, some flights had inaccurate altitude data. The TL and body width values of dolphin images taken during these flights (i.e., pixel images) were not included in the final results since they were inaccurate. However, the BAI values from these pixel images were included in the final analysis. BAI values calculated from the same UAS images of gray whales using raw pixel values and scaled metric values had a perfect linear relationship (Lemos et al., 2020), demonstrating that the BAI values calculated using pixel and scaled images in this study are comparable.

To investigate the accuracy of UAS measurements and account for measurement uncertainty, multiple approaches were taken. First, the coefficient of variation (CV) for TL was calculated separately for scaled and pixel images of dolphins with multiple images included in the final analysis to compare the measurement uncertainty of the UAS. For BAI, the CV was calculated together for scaled and pixel images of dolphins with multiple images included in the final analysis. If a dolphin had its body condition estimated during multiple seasons, its CV for BAI was calculated separately for each season (if each season had multiple images included in the final analysis) since body condition can change over time. Lower CV values translate to more precise estimated measurements for dolphin TL and BAI (Bierlich et al., 2021b). In addition to

CV calculations, one of the dolphins that had his TL estimated in scaled images from multiple UAS surveys was identified as "FB810," a male CESS dolphin that previously had his TL measured during live-capture health assessments in the CES in 1999 (estimated age ~37 y; Fair et al., 2006). Therefore, FB810's estimated TL from the UAS was compared to his measured TL in 1999. Lastly, a male Tamanend's bottlenose dolphin ("SC2303") that stranded on Kiawah Island, South Carolina, on 6 February 2023 was opportunistically measured on a necropsy table using the same UAS and protocol described above. The TL of SC2303 was also measured by the stranding response team, allowing UAS TL estimates at various altitudes to be compared to his true TL. The CV for TL for SC2303 was calculated to compare UAS measurement uncertainty between stranded and free-ranging dolphins in the CES.

Statistical Analysis

To assess if dolphin body condition changes in the CES are influenced by site, season, and age class, a linear mixed effects model was constructed using the 'nlme' package (Pinheiro et al., 2023). The fixed predictor variables were site (Drum Island, Folly River, James Island Creek, or Stono River), season (fall, winter, or spring), and age class (adult or calf), while the response variable was BAI. Dolphin ID was included as a random effect to account for potential pseudo-replication of the same individuals throughout the study period. Model fit was evaluated by assessing the marginal R^2 (R^2_m, the variance explained only by the fixed effects) and the conditional R^2 (R^2_c, the variance explained by both the fixed and random effects; i.e., the whole model) using the package 'MuMIn' in *R*, Version 1.47.5 (Barton, 2023). The linear model assumptions were checked as recommended by Pinheiro & Bates (2006). The *p* value and *F* statistic for each predictor variable were determined using the "anova.lme" function in the 'nlme'

package, and *p* values were considered significant at $\alpha < 0.05$. In addition, a pairwise comparison of estimated marginal means was conducted to determine which groups within each predictor variable were significantly different from one another using the 'emmeans' package (Kuznetsova et al., 2017). All statistical analyses were conducted in *R*, Version 4.3.0 (R Core Team, 2023).

Results

UAS Surveys Summary

In total, 144 land-based UAS body condition surveys were conducted in the CES between September 2022 and May 2023. All four sites were surveyed 36 times each throughout the study period with 12 surveys conducted at each site in fall, winter, and spring. Overall, 426 UAS flights were performed. Almost all of the surveys consisted of three UAS flights (n = 138), but six surveys only had two UAS flights completed due to inclement weather. The average distance surveyed per flight was 5.89 ± 2.24 km, and the average flight time was 17.5 ± 2.4 min. The total UAS flight time throughout the entire study period was approximately 124.1 h.

Overall, 239 dolphin sightings occurred during the study with a total of 562 dolphins observed during these sightings, including repeated observations of the same individuals during multiple sightings. Spatially, Drum Island had the most dolphin sightings (*n* = 96) followed by Stono River (*n* = 58), Folly River (*n* = 57), and James Island Creek (*n* = 28). The number of dolphins observed per site followed the same pattern: Drum Island had the highest number of dolphins observed (*n* = 234) followed by Stono River (*n* = 137), Folly River (*n* = 123), and James Island Creek (*n* = 56). Seasonally, winter had the most dolphin sightings (*n* = 99), fall had the fewest dolphin sightings (*n* = 65), and spring had an intermediate number of dolphin sightings (*n* = 75). Similarly, the most dolphins were observed during winter (*n* = 217), but more

dolphins were observed during fall (n = 179) than spring (n = 166). The average number of dolphins observed per survey followed the same spatial and seasonal trends.

Dolphins exhibited potential behavioral reactions to the UAS during approximately 2.5% of sightings (6/239). These reactions all occurred during low altitude descents for high-resolution imagery (≤ 10 m). The potential behavioral reactions to the UAS included tail-slapping, chuffing, breaching, and swimming belly-up. It is worth noting that some of these responses may have been natural behaviors exhibited by dolphins that were socializing rather than responses to the UAS flying at low altitude.

Final Dataset

In total, 693 images of 194 unique dolphins were extracted from UAS videos. After filtering the images for quality based on the photo selection criteria, 428 images of 174 unique dolphins were included in the final analysis. Sample sizes for the number of dolphins included in the final analysis varied by site, season, and age class (Table 1). Of the 174 dolphins included in the final analysis, 35 had images included from multiple surveys, and, thus, it was possible to estimate how their body condition changed over time. Furthermore, 24 of these 35 dolphins (n_{Calf} = 6; n_{Adult} = 18) had their body condition estimated during two seasons (fall-winter, fall-spring, or winter-spring), and the remaining 11 dolphins had their body condition estimated during multiple surveys within the same season. No dolphins had images included from all three seasons. It is also worth noting that five dolphins were observed at multiple sites throughout the study period, and four of those dolphins had measurements included from multiple sites in the final analysis. These five dolphins were observed at James Island Creek and Stono River (n = 3), James Island Creek and Folly River (n = 1), or Stono and Folly Rivers (n = 1).

444

445 *Photogrammetry and BAI Estimates*

446 Overall, 229 of the 428 images (53.5%) included in the final analysis had accurate UAS
447 altitude data and, thus, had their BAI calculated using scaled metric values. The remaining 199
448 images were pixel images and had their BAI calculated using raw pixel values. The linear model
449 fixed effects (R^2_m) explained 26% of variation in body condition (df = 249). The only random
450 effect in the linear model, Dolphin ID, was large and explained 66% (R^2_c to R^2_m) of body
451 condition variation. The fixed variable with the most significant effect on dolphin BAI was age
452 class (F = 65.27, p < 0.0001, df = 1; Figure 4). Specifically, calves exhibited a significantly
453 larger BAI (n = 30; 23.62 ± 0.68 [mean ± SD]) than adults (n = 144; 21.19 ± 0.30; Table 2).
454 Season also had a significant effect on dolphin BAI (F = 6.84, p = 0.0013, df = 2), although its
455 effect size was much smaller than age class (Figure 4). Dolphin BAI was largest during winter (n
456 = 87; 21.55 ± 0.15), followed by fall (n = 56; 21.37 ± 0.21) and spring (n = 55; 21.14 ± 0.14)
457 (Figure 4). However, significant BAI differences were only found between winter and spring
458 (Table 2). Site did not have a significant effect on dolphin BAI (F = 2.25, p = 0.0833, df = 3),
459 and no significant BAI differences were found between any sites (Figure 4; Table 2). Repeated
460 measurements of 24 dolphins between seasons showed that variation in dolphin body condition
461 over time is individual-specific because BAI remained relatively constant over time for some
462 individuals but fluctuated over time for others (Figure 5). For UAS measurement uncertainty
463 associated with BAI, the mean CV for BAI of the same dolphin in different UAS images from
464 each season was 1.12 ± 0.80% (n = 126; range: 0.00 to 4.53%), with the number of images per
465 dolphin per season ranging from two to 10 images.

A total of 100 unique dolphins were measured in the 229 scaled images, meaning that approximately 58% of the individuals (100/174) included in the final analysis had accurate absolute body measurements reported (vs those that relied on relative pixel measures). The TL and body width-length measurements varied depending on age class (Table 3). The mean CV for TL of the same dolphin in different scaled UAS images was 2.95 ± 2.49% (n = 66; range: 0.00 to 11.31%), with the number of scaled images per individual ranging from two to six. By comparison, the mean CV for TL of the same dolphin in different pixel UAS images was 5.55 ± 5.06% (n = 55; range: 0.06 to 30.12%), with the number of pixel images per individual ranging from two to seven. FB810's measured TL was 247 cm during a health assessment in 1999, and his estimated mean TL was 252.0 ± 6.3 cm based on six scaled UAS images taken between altitudes of 9.2 to 14.2 m during three separate surveys (Figure 6). SC2303's measured TL was 256 cm, and his estimated mean TL was 258.5 ± 2.2 cm based on 11 scaled UAS images taken between altitudes of 9.0 to 19.0 m (Figure 6). The UAS measurement uncertainty for TL measurements was lower for SC2303 (CV = 0.83%) than FB810 (CV = 2.51%), although both were lower than the average CV for TL uncertainty from scaled images of free-ranging dolphins.

Drone Dolphin ID Database

Throughout the study, 194 unique Tamanend's bottlenose dolphins were identified from UAS images based on their distinct skin pigmentation and scarring patterns. These individuals were all added to the Drone Dolphin ID database. Of the 194 dolphins identified for potential body condition assessment, 42 were observed during multiple UAS surveys throughout the study period. On average, these 42 dolphins were observed during 2.64 ± 1.06 sightings (range: 2 to 7 sightings). High-quality dorsal fin photos for photo-ID were taken of 20 different dolphin

individuals opportunistically from land. These dorsal fin photos were added to the Drone Dolphin ID database for the corresponding individual. The NMMF matched 14 dorsal fin photos to known CESS individuals in the Charleston bottlenose dolphin dorsal fin catalogue, and any information about them such as sex, age, and sighting history were included in the Drone Dolphin ID database as well. Of the remaining six dorsal fin photos, two belonged to new calves of known CESS individuals that were sighted for the first time during this study and were subsequently added to the Charleston bottlenose dolphin dorsal fin catalogue. The last four individuals had clean dorsal fins that could not be matched to any known dolphins.

Discussion

This study utilized UAS photogrammetry to quantitatively assess Tamanend's bottlenose dolphin body condition changes over a 9-mo period in the CES using BAI as the body condition metric. Despite substantial individual variation in BAI trends over time, this study identified several over-arching factors associated with variation in dolphin BAI in the CES. Specifically, significant dolphin BAI differences were documented by season between winter and spring and by age class between calves and adults, both of which are consistent with other cetacean species (Lockyer, 2007; Lemos et al., 2020; de Oliveira et al., 2023). No site differences in dolphin BAI were observed despite large variation in habitat quality and anthropogenic impact across sites (McFee & Lipscomb, 2009; McFee et al., 2014; Transue et al., 2023). To our knowledge, this is the first study to use BAI as the body condition metric for a study focused on a small cetacean or odontocete species, further demonstrating the ability of BAI to detect potential body condition differences between individuals in small estuarine cetacean populations. This methodology is a valuable first step toward noninvasively understanding differences in CESS dolphin body

condition on an individual and population level, and it may be combined with biopsy darting and lipidomic analysis moving forward to further understand the relationship between BAI, lipid reserves, and body condition in this population (Sherrill et al., 2024).

Age Class BAI Results

Age class was the most significant predictor of dolphin BAI in the CES, and dolphin calves had higher mean BAI than adults. This suggests that calves have more energy reserves relative to their overall body size than adults, although they likely have more total energy expenditures than adults as well (Rimbach et al., 2021). These findings are consistent with Pacific Coast Feeding Group gray whale calves, which also exhibit the highest average BAI out of any demographic unit in the population (Lemos et al., 2020). Although our sample size was relatively small, six CESS dolphin calves had their BAI evaluated during surveys from multiple seasons, which allowed their body condition to be monitored over time. In general, a trend of decreasing calf body condition over time was observed as four of the six calves had a lower BAI during the second season than that measured for the first. One possible reason for this trend is that calves may be more susceptible to infectious diseases—one of the leading causes of death for bottlenose dolphins in South Carolina (McFee & Lipscomb, 2009)—than adults because they have lower immune heath and cannot fight off infection (McFee et al., 2020). After becoming ill, sick animals may have a reduced appetite which could lead to their body condition deteriorating over time (Kuiken et al., 1994). Another explanation for the trend of decreasing calf BAI over time is that calf BAI becomes more independent of its mother's BAI as the weaning process progresses, which is suspected for humpback whales (Bierlich et al., 2022). However, the weaning process for bottlenose dolphins is quite complex because the exact time that calves start eating fish varies

between individuals, although most begin eating solid food within the first year of birth (Kastelein et al., 2002). Calves usually stop suckling completely by 18 mo, but suckling can last longer as calves under managed care have been documented suckling until they were 37 mo, and wild calves may suckle even longer in some cases (Peddemors et al., 1992; Connor et al., 2000; Kastelein et al., 2002). Since fish consumption begins prior to suckling termination, weaning is a gradual process for calves that is highly variable depending on the exact timing of suckling termination and food independence (Peddemors et al., 1992). Given how variable the weaning process is for bottlenose dolphin calves, this may explain partially why the BAI of some calves increased over time while others decreased.

Calves also may have higher BAI than adults based on how they grow over time. Dolphins in the CES have multiple growth phases, including an early period of rapid growth (0 to 5 wks), a secondary period of slower sustained growth (~6 wks to 7 y), and a rapid growth spurt around the age of sexual maturity (~10 y) (McFee et al., 2009). Based on their growth phases, CESS dolphins most likely prioritize investing energy toward TL growth during the first growth phase but may invest energy toward improving their body condition during the secondary growth phase when the TL growth rate is reduced (McFee et al., 2009). Humpback whale calves initially prioritize TL gain on their breeding grounds after being born, but subsequently invest in improving their body condition on their foraging grounds, further supporting this idea (Christiansen et al., 2016; Bierlich et al., 2022). If this is the case, CESS dolphin calves may attain a high BAI during the secondary growth phase, which peaks at ~6 wks old (McFee et al., 2009). However, as calves' TL increases over time as they continue to grow, they may have less energy reserves relative to their body size, thus causing their BAI to decrease and more closely resemble the generally lower BAI of adults.

Adult dolphins in the CES that had their body condition estimated during multiple seasons did not exhibit any clear trends in regards to how their BAI changed over time. Some individuals had similar BAI over time, others had slight increases or decreases in BAI over time, and a few individuals had large increases or decreases in BAI over time. This suggests that the body condition of adult dolphins in the CES is highly dependent on the individual as different individuals exhibit unique body condition changes over time. The linear model further supports this because Dolphin ID alone (as a random effect) accounted for a majority of dolphin BAI variation in the CES. Numerous factors can influence the body condition of adult cetaceans, including season (Lockyer, 2007; Kastelein et al., 2018; de Oliveira et al., 2023), reproductive status (Christiansen et al., 2016, 2018, 2021; Lemos et al., 2020; Bierlich et al., 2022), and prey availability (Lemos et al., 2020; Stewart et al., 2021; Bierlich et al., 2022; Torres et al., 2022). To better understand how each of these factors may influence CESS dolphin body condition, long-term UAS monitoring and annual estimations of prey availability in the CES are needed.

Seasonal BAI Results

Significant seasonal differences in dolphin BAI were found, indicating that season is associated with dolphin body condition in the CES. Specifically, BAI was significantly higher during winter than spring, but BAI in fall was not significantly different from either winter or spring. This suggests that dolphins in the CES have more energy reserves during winter than spring and may begin accumulating energy reserves for winter in fall. Similar findings have been reported for other small odontocete species as well. For instance, harbor porpoise body condition in the North Atlantic tends to be better in winter than summer when they have thicker blubber and more stored energy reserves, most likely due to increased food consumption in the winter (Lockyer et

al., 2003; Lockyer, 2007; Kastelein et al., 2018). Franciscanas and Guiana dolphins also exhibit better body condition during winter than summer based on UAS photogrammetry (de Oliveira et al., 2023). The findings from these studies support results from the current study and collectively suggest that smaller odontocete species tend to exhibit a better body condition in colder months.

The body condition of small odontocete species may improve during winter because they adjust their dietary behaviors to maintain thermal insulation despite colder water temperatures and resources being scarcer (Lockyer, 2007). To increase their energy reserves and to compensate for these seasonal issues, small odontocetes may increase their food consumption rate during winter or in fall to prepare for winter (Kastelein et al., 2018). As an estuarine ecosystem, the CES serves as an important nursery area for offshore fish species during warmer months as well as a year-round habitat for numerous inshore fish species (Wenner et al., 1984). Many common CESS dolphin prey species such as red drum (*Sciaenops ocellatus*) spawn in the CES during summer and migrate offshore during fall, thus causing resident CESS dolphins to adjust their diets seasonally (Pate & McFee, 2012). During winter and spring, CESS dolphins may consume larger, energy-rich prey that is less abundant, but during summer and fall they sustain themselves on smaller, lower-quality prey that is highly abundant (McCluskey et al., 2016). For instance, star drum (*Stellifer lanceolatus*), an abundant fish species that lives in the estuarine waters of South Carolina year-round, is one of the most prevalent dolphin prey items during winter (67%) but one of the least prevalent prey items during summer (11%) (Wenner et al., 1984; Pate & McFee, 2012). By shifting their dietary preferences to higher-quality, energy-rich prey during winter, CESS dolphins likely increase their blubber thickness and body mass (Lockyer et al., 2003; Kastelein et al., 2018), which is reflected by their higher BAI in winter. The seasonal distribution pattern of CESS dolphins supports this theory because CESS dolphins

604 are concentrated at the mouth of Charleston Harbor during summer and fall when spawning
605 offshore fish are most common, but during winter and spring they are concentrated deep within
606 the harbor and inshore river systems when primarily only year-round estuarine fish remain
607 (Bouchillon et al., 2020).

608 Beyond seasonal dietary shifts, cetacean body condition also varies frequently during
609 reproductive periods (Lockyer, 2007; Miller et al., 2012). Cetacean reproduction requires
610 significant energy investment, particularly for mature females that typically produce, raise, and
611 wean their calves within 1 to 3 y after birth (Lockyer, 1984). For instance, lactating southern
612 right whale (*Eubalaena australis*) females lose approximately 25% of their body volume during
613 the first 3 mo of the breeding season, and lactating and post-weaning gray whales have the
614 lowest BAI (i.e., worst body condition) of any demographic group in their population
615 (Christiansen et al., 2018; Lemos et al., 2020). Small odontocete species also invest significant
616 energy into reproduction as most common bottlenose dolphin mothers produce milk for their
617 calves for 1.5 to 3 y, and calves often stay with their mothers for 3 to 6 y (Shane et al., 1986).
618 Based on neonate sightings and strandings, the CESS dolphin breeding season most likely peaks
619 in spring and early summer (McFee et al., 2014). During the peak breeding season, CESS
620 dolphins may shift their energetic priorities to reproduction instead of survival and
621 thermoregulation. This energetic shift could lead to poorer CESS dolphin body condition in
622 spring and early summer, which would explain why dolphin BAI is significantly higher in winter
623 than in spring. While UAS surveys intentionally were not conducted during summer to minimize
624 the potential of including seasonal resident and transient dolphins in the study (Zolman, 2002),
625 future research conducted during summer would provide important insight into how CESS
626 dolphin body condition changes throughout the entire year.

627

628 *Spatial BAI Results*

629 No significant dolphin body condition differences were detected between the four study sites,
630 indicating that anthropogenic disturbance or habitat quality differences between sites may not
631 influence dolphin body condition in the CES (McFee & Lipscomb, 2009; McFee et al., 2014;
632 Transue et al., 2023). However, it is important to consider that dolphins move throughout the
633 CES, and it is highly unlikely that any animals spend all of their time exclusively within the area
634 of one site. Short-term satellite telemetry of three male CESS dolphins indicated that they have
635 localized ranging patterns ≤ 30 km2 (Balmer et al., 2021), which is a much larger area than the
636 UAS was able to survey. Furthermore, portions of both the Folly and Stono Rivers were included
637 in these dolphins' localized ranges (Balmer et al., 2021), suggesting that considering the Folly
638 and Stono Rivers as separate sites may not be an accurate representation of CESS dolphins'
639 ranging patterns. Although only five dolphins were identified at multiple sites during the study,
640 CESS dolphins are known to move throughout the CES, and their distribution depends on
641 numerous factors, including sex, season, and, potentially, age class (Bouchillon et al., 2020;
642 Balmer et al., 2021). Conducting boat-based UAS body condition surveys is recommended for
643 future studies to better account for these distribution patterns and allow the UAS to follow
644 dolphins for a longer period of time, which was limited by the land-based design of this study.
645 This will further improve our understanding of how habitat differences may influence CESS
646 dolphin body condition, particularly in low salinity habitats that dolphins in the CES have begun
647 using more frequently (Principe et al., 2023), but may have adverse health effects on animals if
648 they remain in these areas long-term (Deming et al., 2020; Duignan et al., 2020).

649

650 *Behavioral Response to the UAS*

651 Overall, dolphins in the CES exhibited few behavioral reactions to the UAS. Notably, these
652 reactions only occurred during low UAS descents (≤ 10 m), suggesting that this altitude may be
653 the threshold at which dolphins in the CES potentially respond to the UAS in flight. However,
654 even when dolphins did react to the UAS, the duration of the response was short as they quickly
655 resumed their prior behavior once the UAS elevated to a higher altitude. This indicates that the
656 disturbance induced by the UAS was minimal. Previous studies that tested the behavioral
657 responses of bottlenose dolphins to the UAS found varying responses depending on the
658 population. In general, different dolphin populations around the world exhibited little to no
659 behavioral responses to the UAS, although most behavioral changes that did occur were between
660 altitudes of 10 to 30 m and were usually brief (Ramos et al., 2018; Fettermann et al., 2019;
661 Castro et al., 2021; Giles et al., 2021). Collectively, these studies indicate that the responses of
662 bottlenose dolphins to the UAS may be population-specific, which has been suggested for
663 different Indo-Pacific humpback dolphin populations in the South China Sea (Serres et al.,
664 2024). Despite not being the primary objective, the findings from this study support the
665 continued use of the UAS to monitor dolphins in the CES. Flying above 10 m is recommended to
666 minimize UAS disturbance.

667

668 *UAS Data Collection: Limitations & Future Recommendations*

669 Overall, this study successfully demonstrated that aerial imagery collected during UAS flights
670 can be used to detect body condition differences in Tamanend's bottlenose dolphins in the CES,
671 which is consistent with other UAS body condition studies of small cetaceans (de Oliveira et al.,
672 2023; Serres et al., 2024). However, since this was a pilot study designed to determine if UAS

aerial photogrammetry could be utilized to evaluate dolphin body condition in the CES, there are numerous ways that the protocol used could be improved to obtain higher-quality data in future monitoring efforts. First, the amount of life history information available about each animal was limited, largely due to the land-based design of the study. Many other UAS cetacean body condition studies have been conducted from a small research vessel over the span of multiple years and employ complementary techniques such as photo-ID and biopsy darting, allowing them to accurately determine many individuals' sex, age class, and reproductive status (Christiansen et al., 2020, 2021; Lemos et al., 2020; Bierlich et al., 2022; Torres et al., 2022). In the present study, no biopsy efforts were attempted, and opportunistic photo-ID images were limited to dolphins that passed close to shore. Therefore, life history information about most of the dolphins in this study was restricted to what could be determined based on UAS video. For sex, adult dolphins were assumed to be female based on the presence of a calf, and males could only be identified if their genitalia were observed in UAS videos during group socio-sexual behaviors. For age class, dolphins could only be assigned as adults or calves based on UAS limitations. However, many studies classify sexually immature sub-adults as a separate age class group (McFee et al., 2009; Cheney et al., 2022). Based on the average adult dolphin TL from scaled UAS images, it is likely that many of the dolphins that were classified as adults were actually subadults. Since subadults may experience different body condition trends than adults because they are still growing, this may have influenced the results. Future UAS studies should attempt to distinguish between calves, subadults, and adults, if possible, potentially using novel UAS methods that accurately quantify the age class of free-ranging dolphins by measuring the distance between the blowhole and dorsal fin to estimate TL (Vivier et al., 2023).

Another challenge in this study was identifying the reproductive status of dolphins. Lactating females could be determined by the presence of a calf, but identifying pregnant, postweaning, or resting females was highly difficult during a 9-mo time period solely using UAS imagery. Previous studies conducted across multiple years have shown that BAI varies greatly depending on female reproductive status (Lemos et al., 2020; Bierlich et al., 2022; Torres et al., 2022), but the effect of reproductive status on CESS dolphin BAI could not be investigated in this study since the reproductive status of most individuals could not be determined. Other than continuing UAS monitoring for multiple years, one solution to address this issue may be using the UAS to identify pregnant dolphins based on their body widths (Cheney et al., 2022). This would improve assignment of dolphins into accurate reproductive classes and allow changes in individual body condition based on reproductive status to be determined, which could help estimate the energetic cost of reproduction for CESS dolphins (Christiansen et al., 2016).

Despite the limited life history information that was available about each dolphin, it is worth highlighting that the Drone Dolphin ID database developed for this study circumvented some of these issues and proved to be a powerful tool for tracking individuals over time and gradually accumulating data about them. Similar to traditional photo-ID studies (Zolman, 2002; Speakman et al., 2010), low altitude high-quality UAS images helped identify the same individuals over time based on their unique scars, skin lesions, teeth rake marks, pigmentation patterns, and other distinctive markings. While previous UAS studies of bottlenose dolphins have used markings to match the same individual in UAS images and photo-ID camera images (Cheney et al., 2022), the current study appears to be the first to use UAS imagery to track dolphin individuals over time based on their distinctive features. Developing a UAS imagery database is particularly useful for monitoring resident dolphin populations, such as CESS

718 dolphins, because many different attributes about individuals can be observed over time such as
719 their movements, site preferences, interactions, behavior, etc. These applications demonstrate the
720 potential of the Drone Dolphin ID database as a comprehensive long-term CESS dolphin
721 monitoring tool; therefore, further developing this database is strongly recommended. In
722 particular, conducting UAS body condition surveys from a small vessel would allow dorsal fin
723 photo-ID images to be collected concurrently with UAS imagery, which could then be used to
724 match dolphins to known animals in the Charleston bottlenose dolphin dorsal fin catalogue
725 (Adams et al., 2006). All of the information about each dolphin could be stored in one
726 comprehensive database containing the individual's dorsal fin image, UAS images showing the
727 animal's distinctive body markings, sighting history, and any other information obtained during
728 health assessments or opportunistic observations such as sex, age, or reproductive status.
729 Other than limited dolphin data, another aspect of the study design that needs to be
730 addressed is the UAS model used. The DJI Air 2S was primarily chosen as the UAS model due
731 to available resources and its being relatively inexpensive (~$1,000 USD). Most UAS cetacean
732 body condition studies have used higher-quality and more expensive UAS models such as the
733 DJI Phantom 3 or 4 Pro (Burnett et al., 2018; Lemos et al., 2020; Arranz et al., 2022; Christie et
734 al., 2022; Torres et al., 2022; de Oliveira et al., 2023), an APH-22 hexacopter (Durban et al.,
735 2015, 2016, 2021; Christiansen et al., 2020; Fearnbach et al., 2020; Stewart et al., 2021), or a DJI
736 Inspire 1 or 2 equipped with a Zenmuse X5 camera (Christiansen et al., 2018, 2020, 2021;
737 Arranz et al., 2022; Bierlich et al., 2022; Serres et al., 2024). As a result, previous studies of
738 small cetaceans have been able to fly at higher altitudes (15 to 60 m) while still collecting high-
739 quality images that can be used for photogrammetry and body condition assessment (Arranz et
740 al., 2022; Cheney et al., 2022; Christie et al., 2022; de Oliveira et al., 2023; Serres et al., 2024).

Due to the relatively lower quality of the DJI Air 2S camera, the UAS in this study was typically flown at lower altitudes (9.2 to 15 m) to obtain high-quality imagery that could be used to assess body condition and identify dolphin individuals. This was also necessary due to poor water clarity in the CES, which made viewing dolphins from the UAS difficult even if the animals were just below the surface (Principe et al., 2023).

Another issue with the UAS in this study was the lack of consistently accurate altitude data from the onboard barometer, which caused only ~54% of images included in the final analysis to be scaled. As a result, estimated body measurements were only available for a subset of the dolphins in this study. However, the main goal of this study was to assess dolphin body condition in the CES, so accurate body measurements would not have been any better than the BAI body ratio for this purpose (Serres et al., 2024). If estimated morphometric measurements are desired for future studies, a UAS with lower measurement uncertainty should be used or a laser altimeter should be attached to the DJI Air 2S (Durban et al., 2015, 2016, 2021; Dawson et al., 2017; Christiansen et al., 2018, 2020, 2021; Bierlich et al., 2022; Ramos et al., 2022; Torres et al., 2022). For body condition assessment, the DJI Air 2S did have a higher mean measurement uncertainty for BAI (CV = 1.12%) compared to other higher-quality UASs used in baleen whale body condition studies such as the Inspire 1 Pro (CV = 0.12%) and the Phantom 4 Pro (CV = 0.91%), although it was lower than the measurement uncertainty associated with BAI for the Phantom 4 and the Phantom 3 Pro (CV = 2.97%) (Bierlich et al., 2022; Torres et al., 2022). This could be due to the Phantom 4 and Phantom 3 Pro collecting imagery at higher altitudes between 20 to 36 m (Torres et al., 2022), whereas the imagery in this study was collected at lower altitudes. BAI is known to have high precision and low measurement uncertainty compared to other body condition metrics (Bierlich et al., 2021b), which appears to

be consistent for the DJI Air 2S as well. Since measurement uncertainty is dependent on the camera, focal length lens, and altimeter (Bierlich et al., 2021a), switching to a different UAS model with a higher-quality camera may help reduce BAI measurement uncertainty in future dolphin body condition studies in the CES.

Conclusions

In conclusion, the results from this study demonstrate that UASs can be used to assess the BAI of a small cetacean species and that dolphin BAI in the CES varies based on season and age class despite high individual variation in body condition over time. These findings are generally consistent with other cetacean species, although more UAS studies to date have focused on large whale species rather than small odontocete species. Based on the success of this study, it is strongly recommended that other studies employing the UAS to study cetacean body condition use BAI as their body condition metric. Since BAI facilitates easy body condition comparisons within and between populations, the data from this study could be used to make comparisons between the body condition of CESS dolphins to other Tamanend's bottlenose dolphin populations such as coastal dolphins in South Carolina (Zolman, 2002; Speakman et al., 2010; Laska et al., 2011). As such, the findings from this study provide an important baseline of dolphin body condition in the CES by establishing a relevant BAI range for this population. Moving forward, understanding how dolphin BAI changes in response to environmental or anthropogenic stressors will be important for understanding how stressors influence the health of the CESS population. Boat-based UAS surveys are also recommended for future studies to collect camera photo-ID and UAS images concurrently, which would improve identification of known CESS dolphins and help track how their body condition changes over time. Given that

dolphins in the CES exhibit low overall responsiveness to UAS flights and the results from this study fill crucial knowledge gaps about free-ranging dolphins in this population, the continued use of the UAS to monitor CESS dolphins moving forward is strongly supported. Despite some limitations, this study demonstrates that the UAS can be used as an inexpensive, noninvasive method to monitor the health of dolphins in the CES over time.

Acknowledgements

The scientific results and conclusions, as well as any opinions expressed herein, are those of the author(s) and do not necessarily reflect the views of NOAA or the U.S. Department of Commerce. The mention of any commercial product is not meant as an endorsement by the Agency or Department. This study was conducted under the National Marine Fisheries Service Permit Number 21938-03. After being reviewed by the College of Charleston's Institutional Animal Care and Use Committee (IACUC), it was determined that the study was field observational in nature and no IACUC permission was required. Funding for this project was in part provided by two research grants awarded by the Graduate School at the College of Charleston. The authors would like to thank the National Marine Mammal Foundation, specifically Todd Speakman, for comparing dorsal fin photos collected during this study to animals in their database. In addition, the authors would like to thank everyone who assisted with UAS surveys throughout the study, including Kerryanne Litzenberg, Hannah Korper, and Gautam Ghosh. In addition, the authors would like to provide special thanks to Libby Smith for granting access to her dock on James Island Creek to conduct UAS surveys during the study. Lastly, thank you to the Lowcountry Marine Mammal Network members (Megan Krzewinski

and Nicole Principe) and NOAA volunteers (Bonnie Ertel) for collecting SC2303 and assisting with UAS data collection of this animal.

Literature Cited

Adams, J. D., Speakman, T., Zolman, E., & Schwacke, L. H. (2006). Automating image matching, cataloging, and analysis for photo-identification research. *Aquatic Mammals*, *32*(3), 374. https://doi.org/10.1578/AM.32.3.2006.374

Adams, J. D., Speakman, T., Zolman, E., & Schwacke, L. H. (2006). Automating image matching, cataloging, and analysis for photo-identification research. *Aquatic Mammals*, *32*(3), 374. https://doi.org/10.1578/AM.32.3.2006.374

Arranz, P., Christiansen, F., Glarou, M., Gero, S., Visser, F., Oudejans, M. G., Aguilar de Soto, N., & Sprogis, K. (2022). Body condition and allometry of free-ranging short-finned pilot whales in the North Atlantic. *Sustainability*, *14*(22), 14787. https://doi.org/10.3390/su142214787

Atkinson, S., Rogan, A., Baker, C. S., Dagdag, R., Redlinger, M., Polinski, J., Urban, J., Sremba, A., Branson, M., Mashburn, K., Pallin, L., Klink, A., Steel, D., Bortz, E., & Kerr, I. (2021). Genetic, endocrine, and microbiological assessments of blue, humpback and killer whale health using unoccupied aerial systems. *Wildlife Society Bulletin*, *45*(4), 654-669. https://doi.org/10.1002/wsb.1240

Balmer, B. C., McCulloch, S. D., Speakman, T. R., Foster, J., Hansen, L. J., McFee, W. E., & Bossart, G. D. (2021). Comparison of Short-Term Satellite Telemetry and Long-Term Photographic-Identification for Assessing Ranging Patterns of Individual Common Bottlenose Dolphins (Tursiops truncatus) in the Waters Around Charleston, South Carolina, USA. *Aquatic Mammals*, *47*(4), 355-361. https://doi.org/10.1578/AM.47.4.2021.355

Barton, K. (2023). MuMIn: Multi-Model Inference. R package version 1.47.5, https://CRAN.R-project.org/package=MuMIn.

Bierlich, K. C., Hewitt, J., Bird, C. N., Schick, R. S., Friedlaender, A., Torres, L. G., Dale, J., Goldbogen, J., Read, A. J., Calambokidis, J., & Johnston, D. W. (2021a). Comparing uncertainty associated with 1-, 2-, and 3D aerial photogrammetry-based body condition measurements of baleen whales. *Frontiers in Marine Science*, 1729. https://doi.org/10.3389/fmars.2021.749943

Bierlich, K. C., Schick, R. S., Hewitt, J., Dale, J., Goldbogen, J. A., Friedlaender, A. S., & Johnston, D. W. (2021b). Bayesian approach for predicting photogrammetric uncertainty in morphometric measurements derived from drones. *Marine Ecology Progress Series*, *673*, 193-210. https://doi.org/10.3354/meps13814

Bierlich, K. C., Hewitt, J., Schick, R. S., Pallin, L., Dale, J., Friedlaender, A. S., Christiansen, F., Sprogis, K. R., Dawn, A. H., Bird, C. N., Larsen, G. D., Nichols, R., Shero, M. R., Goldbogen, J., Read, A. J., & Johnston, D. W. (2022). Seasonal gain in body condition of

foraging humpback whales along the Western Antarctic Peninsula. *Frontiers in Marine Science*, *9*, 1036860. https://doi.org/10.3389/fmars.2022.1036860

Bird, C. N., & Bierlich, K. C. (2020). CollatriX: A GUI to collate MorphoMetriX outputs. *Journal of Open Source Software*, *5*(51), 2328. https://doi.org/10.21105/joss.02328

Bouchillon, H., Levine, N. S., & Fair, P. A. (2020). GIS Investigation of the relationship of sex and season on the population distribution of common bottlenose dolphins (Tursiops truncatus) in Charleston, South Carolina. *International Journal of Geographical Information Science*, *34*(8), 1552-1566. https://doi.org/10.1080/13658816.2019.1615068

Brodie, P. F. (1975). Cetacean energetics, an overview of intraspecific size variation. *Ecology*, *56*(1), 152-161. https://doi.org/10.2307/1935307

Burnett, J. D., Lemos, L., Barlow, D., Wing, M. G., Chandler, T., & Torres, L. G. (2018). Estimating morphometric attributes of baleen whales with photogrammetry from small UASs: A case study with blue and gray whales. *Marine Mammal Science*, *35*(1), 108-139. https://doi.org/10.1111/mms.12527

Castro, J., Borges, F. O., Cid, A., Laborde, M. I., Rosa, R., & Pearson, H. C. (2021). Assessing the behavioural responses of small cetaceans to unmanned aerial vehicles. *Remote Sensing*, *13*(1), 156. https://doi.org/10.3390/rs13010156

Cheney, B. J., Dale, J., Thompson, P. M., & Quick, N. J. (2022). Spy in the sky: A method to identify pregnant small cetaceans. *Remote Sensing in Ecology and Conservation*, *8*(4), 492-505. https://doi.org/10.1002/rse2.258

Christiansen, F., Víkingsson, G. A., Rasmussen, M. H., & Lusseau, D. (2014). Female body condition affects foetal growth in a capital breeding mysticete. *Functional Ecology*, *28*(3), 579-588. https://doi.org/10.1111/1365-2435.12200

Christiansen, F., Dujon, A. M., Sprogis, K. R., Arnould, J. P., & Bejder, L. (2016). Noninvasive unmanned aerial vehicle provides estimates of the energetic cost of reproduction in humpback whales. *Ecosphere*, *7*(10), e01468. http://dx.doi.org/10.1002/ecs2.1468

Christiansen, F., Vivier, F., Charlton, C., Ward, R., Amerson, A., Burnell, S., & Bejder, L. (2018). Maternal body size and condition determine calf growth rates in southern right whales. *Marine Ecology Progress Series*, *592*, 267-281. https://doi.org/10.3354/meps12522

Christiansen, F., Rodríguez-González, F., Martínez-Aguilar, S., Urbán, J., Swartz, S., Warick, H., Vivier, F., & Bejder, L. (2021). Poor body condition associated with an unusual mortality event in gray whales. *Marine Ecology Progress Series*, *658*, 237-252. https://doi.org/10.3354/meps13585

Christie, A. I., Colefax, A. P., & Cagnazzi, D. (2022). Feasibility of Using Small UAVs to Derive Morphometric Measurements of Australian Snubfin (Orcaella heinsohni) and Humpback (Sousa sahulensis) Dolphins. *Remote Sensing*, *14*(1), 21. https://doi.org/10.3390/rs14010021

Connor, R. C., & Wells, R. (2000). The bottlenose dolphin: social relationship in a fission-fusion society. In J. Mann, R. C. Connor, P. L. Tyack, H. Whitehead (Eds.), *Cetacean societies: field studies of whales and dolphins* (pp. 91-126). The University of Chicago Press.

Costa, A. P., Mcfee, W., Wilcox, L. A., Archer, F. I., & Rosel, P. E. (2022). The common bottlenose dolphin (Tursiops truncatus) ecotypes of the western North Atlantic revisited: an integrative taxonomic investigation supports the presence of distinct species. *Zoological Journal of the Linnean Society*, *196*(4), 1608-1636.

Dawson, S. M., Bowman, M. H., Leunissen, E., & Sirguey, P. (2017). Inexpensive aerial photogrammetry for studies of whales and large marine animals. *Frontiers in Marine Science*, *4*, 366. https://doi.org/10.3389/fmars.2017.00366

de Oliveira, L. L., Andriolo, A., Cremer, M. J., & Zerbini, A. N. (2023). Aerial photogrammetry techniques using drones to estimate morphometric measurements and body condition in South American small cetaceans. *Marine Mammal Science*, *39*(3), 811-829. https://doi.org/10.1111/mms.13011

Deming, A. C., Wingers, N. L., Moore, D. P., Rotstein, D., Wells, R. S., Ewing, R., Hobanbosi, M. R., & Carmichael, R. H. (2020). Health impacts and recovery from prolonged freshwater exposure in a common bottlenose dolphin (Tursiops truncatus). *Frontiers in Veterinary Science*, *7*, 235. https://doi.org/10.3389/fvets.2020.00235

Duignan, P. J., Stephens, N. S., & Robb, K. (2020). Fresh water skin disease in dolphins: a case definition based on pathology and environmental factors in Australia. *Scientific Reports*, *10*(1), 21979. https://doi.org/10.1038/s41598-020-78858-2

Durban, J. W., Fearnbach, H., Barrett-Lennard, L. G., Perryman, W. L., & Leroi, D. J. (2015). Photogrammetry of killer whales using a small hexacopter launched at sea. *Journal of Unmanned Vehicle Systems*, *3*(3), 131-135. https://doi.org/10.1139/juvs-2015-0020

Durban, J. W., Moore, M. J., Chiang, G., Hickmott, L. S., Bocconcelli, A., Howes, G., Bahamonde, P. A., Perryman, W. L., & LeRoi, D. J. (2016). Photogrammetry of blue whales with an unmanned hexacopter. *Marine Mammal Science*, *32*(4), 1510-1515. https://doi.org/10.1111/mms.12328

Durban, J. W., Fearnbach, H., Paredes, A., Hickmott, L. S., & LeRoi, D. J. (2021). Size and body condition of sympatric killer whale ecotypes around the Antarctic Peninsula. *Marine Ecology Progress Series*, *677*, 209-217. https://doi.org/10.3354/meps13866

Fair, P. A., Adams, J. D., Zolman, E., McCulloch, S. D., Goldstein, J. D., Murdoch, M. E., Varela, R., Hansen, L., Townsend, F., Kucklick, J., Bryan, C., Christopher, S., Pugh, R., & Bossart, G. D. (2006). *Protocols for conducting dolphin capture-release health assessment studies* (NOAA Technical Memorandum NOS NCCOS 49). National Oceanic and Atmospheric Administration, U.S. Department of Commerce.

Fearnbach, H., Durban, J. W., Ellifrit, D. K., & Balcomb, K. C. (2018). Using aerial photogrammetry to detect changes in body condition of endangered southern resident killer whales. *Endangered Species Research*, *35*, 175-180. https://doi.org/10.3354/esr00883

Fearnbach, H., Durban, J. W., Barrett-Lennard, L. G., Ellifrit, D. K., & Balcomb III, K. C. (2020). Evaluating the power of photogrammetry for monitoring killer whale body condition. *Marine Mammal Science*, *36*(1), 359-364. http://dx.doi.org/10.1111/mms.12642

Fettermann, T., Fiori, L., Bader, M., Doshi, A., Breen, D., Stockin, K. A., & Bollard, B. (2019). Behaviour reactions of bottlenose dolphins (Tursiops truncatus) to multirotor Unmanned

Aerial Vehicles (UAVs). *Scientific Reports*, *9*(1), 8558. https://doi.org/10.1038/s41598-019-44976-9

Gallagher, D., Visser, M., Sepulveda, D., Pierson, R. N., Harris, T., & Heymsfield, S. B. (1996). How useful is body mass index for comparison of body fatness across age, sex, and ethnic groups?. *American journal of epidemiology*, *143*(3), 228-239.

Giles, A. B., Butcher, P. A., Colefax, A. P., Pagendam, D. E., Mayjor, M., & Kelaher, B. P. (2021). Responses of bottlenose dolphins (Tursiops spp.) to small drones. *Aquatic conservation: marine and freshwater ecosystems*, *31*(3), 677-684. https://doi.org/10.1002/aqc.3440

Hartel, E. F., Constantine, R., & Torres, L. G. (2014). Changes in habitat use patterns by bottlenose dolphins over a 10-year period render static management boundaries ineffective. *Aquatic Conservation: Marine and Freshwater Ecosystems*, *25*(5), 701-711. https://doi.org/10.1002/aqc.2465

Hodgson, J. C., Baylis, S. M., Mott, R., Herrod, A., & Clarke, R. H. (2016). Precision wildlife monitoring using unmanned aerial vehicles. *Scientific reports*, *6*(1), 1-7. https://doi.org/10.1038/srep22574

IJsseldijk, L. L., Hessing, S., Mairo, A., Ten Doeschate, M. T., Treep, J., van den Broek, J., Keijl, G. O., Siebert, U., Heesterbeek, H., Gröne, A., & Leopold, M. F. (2021). Nutritional status and prey energy density govern reproductive success in a small cetacean. *Scientific reports*, *11*(1), 19201. https://doi.org/10.1038/s41598-021-98629-x

Kastelein, R. A., Vaughan, N., Walton, S., & Wiepkema, P. R. (2002). Food intake and body measurements of Atlantic bottlenose dolphins (Tursiops truncates) in captivity. *Marine Environmental Research*, *53*(2), 199-218. https://doi.org/10.1016/S0141-1136(01)00123-4

Kastelein, R. A., Helder-Hoek, L., & Jennings, N. (2018). Seasonal Changes in Food Consumption, Respiration Rate, and Body Condition of a Male Harbor Porpoise (Phocoena phocoena). *Aquatic Mammals*, *44*(1). https://doi.org/10.1578/AM.44.1.2018.76

Kershaw, J. L., Ramp, C. A., Sears, R., Plourde, S., Brosset, P., Miller, P. J., & Hall, A. J. (2021). Declining reproductive success in the Gulf of St. Lawrence's humpback whales (Megaptera novaeangliae) reflects ecosystem shifts on their feeding grounds. *Global Change Biology*, *27*(5), 1027-1041. https://doi.org/10.1111/gcb.15466

Kuiken, T., Bennett, P. M., Allchin, C. R., Kirkwood, J. K., Baker, J. R., Lockyer, C. H., Walton, M. J., & Sheldrick, M. C. (1994). PCBs, cause of death and body condition in harbour porpoises (Phocoena phocoena) from British waters. *Aquatic Toxicology*, *28*(1-2), 13-28.

Kuznetsova, A., Brockhoff, P. B., & Christensen, R. H. (2017). lmerTest package: tests in linear mixed effects models. *Journal of statistical software*, *82*, 1-26.

Laska, D., Speakman, T., & Fair, P. A. (2011). Community overlap of bottlenose dolphins (Tursiops truncatus) found in coastal waters near Charleston, South Carolina. *Journal of Marine Animals and Their Ecology*, *4*(2), 10-18.

Lemos, L., Burnett, J. D., Chandler, T. E., Sumich, J. L., & Torres, L. G. (2020). Intra-and inter-annual variation in gray whale body condition on a foraging ground. *Ecosphere*, *11*(4), e03094. https://doi.org/10.1002/ecs2.3094

Lockyer, C. (1984). Review of baleen whale (Mysticeti) reproduction and implications for management. *Reports of the International Whaling Commission*, *6*, 27-50.

Lockyer, C. (2007). All creatures great and smaller: a study in cetacean life history energetics. *Journal of the Marine Biological Association of the United Kingdom*, *87*(4), 1035-1045. https://doi.org/10.1017/S0025315407054720

Lockyer, C., Desportes, G., Hansen, K., Labberté, S., & Siebert, U. (2003). Monitoring growth and energy utilisation of the harbour porpoise (Phocoena phocoena) in human care. *NAMMCO Scientific Publications*, *5*, 107-120.

Mascie-Taylor, C. G., & Goto, R. (2007). Human variation and body mass index: a review of the universality of BMI cut-offs, gender and urban-rural differences, and secular changes. *Journal of Physiological Anthropology*. *26*(2), 109-112. https://doi.org/10.2114/jpa2.26.109

McCluskey, S. M., Bejder, L., & Loneragan, N. R. (2016). Dolphin prey availability and calorific value in an estuarine and coastal environment. *Frontiers in Marine Science*, *3*, 30. https://doi.org/10.3389/fmars.2016.00030

McFee, W. E., & Lipscomb, T. P. (2009). Major pathologic findings and probable causes of mortality in bottlenose dolphins stranded in South Carolina from 1993 to 2006. *Journal of Wildlife Diseases*, *45*(3), 575-593. https://doi.org/10.7589/0090-3558-45.3.575

McFee, W. E., Schwacke, J. H., Stolen, M. K., Mullin, K. D., & Schwacke, L. H. (2010). Investigation of growth phases for bottlenose dolphins using a Bayesian modeling approach. *Marine Mammal Science*, *26*(1), 67-85. https://doi.org/10.1578/AM.38.1.2012.17

McFee, W. E., Speakman, T. R., Balthis, L., Adams, J. D., & Zolman, E. S. (2014). Reproductive seasonality of a recently designated bottlenose dolphin stock near Charleston, South Carolina, USA. *Marine Mammal Science*, *30*(2), 528-543. https://doi.org/10.1111/mms.12055

McFee, W. E., Wu, D., Colegrove, K., Terio, K., Balthis, L., & Young, R. (2020). Occurrence of Brucella ceti in stranded bottlenose dolphins Tursiops truncatus coincides with calving season. *Diseases of Aquatic Organisms*, *141*, 185-193. https://doi.org/10.3354/dao03526

McHugh, K. A., Allen, J. B., Barleycorn, A. A., & Wells, R. S. (2011). Natal philopatry, ranging behavior, and habitat selection of juvenile bottlenose dolphins in Sarasota Bay, Florida. *Journal of Mammalogy*, *92*(6), 1298-1313. https://doi.org/10.1644/11-MAMM-A-026.1

Miller, C. A., Best, P. B., Perryman, W. L., Baumgartner, M. F., & Moore, M. J. (2012). Body shape changes associated with reproductive status, nutritive condition and growth in right whales Eubalaena glacialis and E. australis. *Marine Ecology Progress Series*, *459*, 135-156. https://doi.org/10.3354/meps09675

Noren, S. R. (2008). Infant carrying behaviour in dolphins: costly parental care in an aquatic environment. *Functional Ecology*, *22*(2), 284-288. https://doi.org/10.1111/j.1365-2435.2007.01354.x

Nowacek, D. P., Christiansen, F., Bejder, L., Goldbogen, J. A., & Friedlaender, A. S. (2016). Studying cetacean behaviour: new technological approaches and conservation applications. *Animal behaviour*, *120*, 235-244. https://doi.org/10.1016/j.anbehav.2016.07.019

Owen, E. C., Wells, R. S., & Hofmann, S. (2002). Ranging and association patterns of paired and unpaired adult male Atlantic bottlenose dolphins, Tursiops truncatus, in Sarasota, Florida, provide no evidence for alternative male strategies. *Canadian Journal of Zoology*, *80*(12), 2072-2089. https://doi.org/10.1139/Z02-195

Pate, S. M., & McFee, W. E. (2012). Prey species of bottlenose dolphins (Tursiops truncatus) from South Carolina waters. *Southeastern Naturalist*, *11*(1), 1-22. https://doi.org/10.1656/058.011.0101

Peddemors, V. M., Fothergill, M., & Cockcroft, V. G. (1992). Feeding and growth in a captive-born bottlenose dolphin Tursiops truncatus. *African Zoology*, *27*(2), 74-80.

Peig, J., & Green, A. J. (2009). New perspectives for estimating body condition from mass/length data: the scaled mass index as an alternative method. *Oikos*, *118*(12), 1883-1891. https://doi.org/10.1111/j.1600-0706.2009.17643.x

Pinheiro, J. C., & Bates, D. M. (Eds). (2006). *Mixed-effects models in S and S-PLUS*. Springer Publishing.

Pinheiro J, Bates D, R Core Team (2023). *nlme: Linear and Nonlinear Mixed Effects Models*. R package version 3.1-162, https://CRAN.R-project.org/package=nlme

Principe, N., McFee, W., Levine, N., Balmer, B., & Ballenger, J. (2023). Using Unoccupied Aerial Systems (UASs) to Determine the Distribution Patterns of Tamanend's Bottlenose Dolphins (Tursiops erebennus) across Varying Salinities in Charleston, South Carolina. *Drones*, *7*(12), 689. https://doi.org/10.3390/drones7120689

R Core Team (2023). _R: A Language and Environment for Statistical Computing_. R Foundation for Statistical Computing, Vienna, Austria. <https://www.R-project.org/.

Ramos, E. A., Maloney, B., Magnasco, M. O., & Reiss, D. (2018). Bottlenose dolphins and Antillean manatees respond to small multi-rotor unmanned aerial systems. *Frontiers in Marine Science*, *5*, 316. https://doi.org/10.3389/fmars.2018.00316

Ramos, E. A., Landeo-Yauri, S., Castelblanco-Martínez, N., Arreola, M. R., Quade, A. H., & Rieucau, G. (2022). Drone-based photogrammetry assessments of body size and body condition of Antillean manatees. *Mammalian Biology*, 1-15. https://doi.org/10.1007/s42991-022-00228-4

Rimbach, R., Amireh, A., Allen, A., Hare, B., Guarino, E., Kaufman, C., Salomons, H., & Pontzer, H. (2021). Total energy expenditure of bottlenose dolphins (Tursiops truncatus) of different ages. *Journal of Experimental Biology*, *224*(15), jeb242218.

Serres, A., Lin, W., Liu, B., Chen, S., & Li, S. (2024). Skinny dolphins: Can poor body condition explain population decline in Indo-Pacific humpback dolphins (Sousa chinensis)?. *Science of The Total Environment*, *917*, 170401. https://doi.org/10.1016/j.scitotenv.2024.170401

Shane, S. H., Wells, R. S., & Wursig, B. (1986). Ecology, behavior and social organization of the bottlenose dolphin: a review. *Marine Mammal Science*, *2*(1), 34–63.

Sherrill, M., Bernier-Graveline, A., Ewald, J., Pang, Z., Moisan, M., Marzelière, M., Muzzy, M., Romano, T. A., Michaud, R., & Verreault, J. (2024). Scaled mass index derived from aerial photogrammetry associated with predicted metabolic pathway disruptions in free-ranging St. Lawrence Estuary belugas. *Frontiers in Marine Science*, *11*, 1360374. https://doi.org/10.3389/fmars.2024.1360374

Silventoinen, K., Jelenkovic, A., Sund, R., Yokoyama, Y., Hur, Y. M., Cozen, W., Hwang, A. E., Mack, T. M., Honda, C., Inui, F., Iwatani, Y., Watanabe, M., Tomizawa, R., Pietiläinen, K. H., Rissanen, A., Siribaddana, S. H., Hotopf, M., Sumathipala, A., Rijsdijk, F., Tan, Q., ... & Kaprio, J. (2017). Differences in genetic and environmental variation in adult BMI by sex, age, time period, and region: an individual-based pooled analysis of 40 twin cohorts. *The American journal of clinical nutrition*, *106*(2), 457-466. https://doi.org/10.3945/ajcn.117.153643

Speakman, T., Zolman, E., Adams, J., Defran, R. H., Laska, D., Schwacke, L., Craigie, J., & Fair, P. (2006). *Temporal and spatial aspects of bottlenose dolphin occurrence in coastal and estuarine waters near Charleston, South Carolina* (NOAA Technical Memorandum NOS-NCCOS-37). National Oceanic and Atmospheric Administration, U.S. Department of Commerce.

Speakman, T. R., Lane, S. M., Schwacke, L. H., Fair, P. A., & Zolman, E. S. (2010). Mark-recapture estimates of seasonal abundance and survivorship for bottlenose dolphins (Tursiops truncatus) near Charleston, South Carolina, USA. *Journal of Cetacean Research and Management*, *11*(2), 153-162.

Sprogis, K. R., Raudino, H. C., Rankin, R., MacLeod, C. D., & Bejder, L. (2016). Home range size of adult Indo-Pacific bottlenose dolphins (Tursiops aduncus) in a coastal and estuarine system is habitat and sex-specific. *Marine Mammal Science*, *32*(1), 287-308. https://doi.org/10.1111/mms.12260

Stewart, J. D., Durban, J. W., Fearnbach, H., Barrett-Lennard, L. G., Casler, P. K., Ward, E. J., & Dapp, D. R. (2021). Survival of the fattest: linking body condition to prey availability and survivorship of killer whales. *Ecosphere*, *12*(8), e03660. https://doi.org/10.1002/ecs2.3660

Torres, W. I., & Bierlich, K. C. (2020). MorphoMetriX: a photogrammetric measurement GUI for morphometric analysis of megafauna. *Journal of Open Source Software*, *5*(45), 1825. https://doi.org/10.21105/joss.01825

Torres, L. G., Bird, C. N., Rodríguez-González, F., Christiansen, F., Bejder, L., Lemos, L., Urban R, J., Swartz, S., Willoughby, A., Hewitt, J., & Bierlich, K. C. (2022). Range-wide comparison of gray whale body condition reveals contrasting sub-population health characteristics and vulnerability to environmental change. *Frontiers in Marine Science*, 511. https://doi.org/10.3389/fmars.2022.867258

Transue, L., Monczak, A., Tribble, C., Marian, A., Fair, P., Ballenger, J., Balmer, B., & Montie, E. W. (2023). The Biological and Anthropogenic Soundscape of an Urbanized Port–the Charleston Harbor Estuary, South Carolina, USA. *Plos One*, *18*(4), e0283848. https://doi.org/10.1371/journal.pone.0283848

United States Environmental Protection Agency (U.S. EPA). (2021). *Superfund Sites in Reuse in South Carolina*. *US EPA*. https://www.epa.gov/superfund-redevelopment-initiative/superfund-sites-reuse-south-carolina#calhoun

Van Dolah, R. F., Wendt, P. H., & Wenner, E. L. (1990). A physical and ecological characterization of the Charleston Harbor Estuarine System. *Marine Resources Division, South Carolina Wildlife and Marine Resources Department*.

Varlik, B. (2019). *Total Maximum Daily Load: James Island Creek-Stations RT-052098, JIC1, and JIC2 in Hydrologic Unit Codes 030502020202 and 030502010605* (SCDHEC Technical Document 002-2020). SCDHEC Bureau of Water.

Vivier, F., Wells, R. S., Hill, M. C., Yano, K. M., Bradford, A. L., Leunissen, E. M., Pacini, A., Booth, C. G., Rocho-Levine, J., Currie, J. J., Patton, P. T., & Bejder, L. (2023). Quantifying the age structure of free-ranging delphinid populations: Testing the accuracy of Unoccupied Aerial System photogrammetry. *Ecology and Evolution*, *13*(6), e10082. https://doi.org/10.1002/ece3.10082

Waring, G. T., Josephson, E., Maze-Foley, K., & Rosel, P. E. (2009). *US Atlantic and Gulf of Mexico marine mammal stock assessments—2010* (NOAA Technical Memorandum NMFS-NE-219). National Oceanic and Atmospheric Administration, U.S. Department of Commerce.

Wells, R. S., Scott, M. D., & Irvine, A. B. (1987). The social structure of free-ranging bottlenose dolphins. In H. H. Genoways (Eds.), *Current mammalogy* (pp. 247-305). Plenum Press.

Wenner, E. L., Coon III, W. P., Shealy Jr, M. H., & Sandifer, P. A. (1984). *A five-year study of seasonal distribution and abundance of fishes and decapod crustaceans in the Cooper River and Charleston Harbor, South Carolina, prior to diversion* (NOAA Technical Report NMFS SSRF-782). National Oceanic and Atmospheric Administration, U.S. Department of Commerce.

Zolman, E. S. (2002). Residence patterns of bottlenose dolphins (Tursiops truncatus) in the Stono River estuary, Charleston County, South Carolina, USA. *Marine Mammal Science*, *18*(4), 879-892. https://doi.org/10.1111/j.1748-7692.2002.tb01079.x

Tables & Figures

Table 1. Sample sizes for the number of Tamanend's bottlenose dolphins (*Tursiops erebennus*) that had images included in the final analysis organized by site, season, and age class. Dolphins that had images included in the final analysis from multiple surveys were counted separately for each survey.

	Season						
	Fall		Winter		Spring		
Site	Adult	Calf	Adult	Calf	Adult	Calf	Total
Drum Island	18	0	35	9	17	4	83
Folly River	10	2	15	3	14	6	50
James Island Creek	11	3	13	0	3	1	31
Stono River	9	6	22	3	13	3	56
Total	48	11	85	15	47	14	220

Table 2. Pairwise comparisons of estimated marginal means for the linear mixed effects model for Tamanend's bottlenose dolphin BAI in the CES based on the variables site, season, and age class. Significant pairwise comparisons ($p < 0.05$) are bold.

Contrast	Estimate	SE	*df*	*t*-value	*p*
Drum Island, Folly River	0.679	0.282	249	2.407	0.0784
Drum Island, James Island Creek	0.264	0.292	249	0.902	0.8036
Drum Island, Stono River	0.119	0.261	249	0.456	0.9684
Folly River, James Island Creek	-0.416	0.266	249	-1.561	0.4028
Folly River, Stono River	-0.560	0.264	249	-2.119	0.1498
James Island Creek, Stono River	-0.145	0.247	249	-0.587	0.936
Fall, Winter	0.236	0.144	249	1.642	0.2300
Fall, Spring	-0.176	0.146	249	-1.210	0.4482
Spring, Winter	-0.412	0.112	249	-3.687	**0.0008**
Adult, Calf	-2.430	0.301	172	-8.079	**< 0.0001**

Table 1. UAS measurements of Tamanend's bottlenose dolphin total length (TL) and body widths taken at 10% width intervals of TL for animals that had scaled images. The mean ± SD is reported for each measurement. In the sample size column, the first number indicates the sample size for each group, while the number in parentheses indicates the number of individuals that had multiple images included in the final analysis and, thus, are contributing to the SD.

Class	Sample Size	UAS Measurement (cm)				
		Total Length	10% Width	20% Width	30% Width	40% Width
Calf	18 (8)	149.9 ± 5.5	14.5 ± 1.4	23.0 ± 1.5	26.7 ± 1.0	27.1 ± 1.6
Adult (All)	88 (63)	220.6 ± 6.5	19.4 ± 1.5	30.5 ± 1.2	35.4 ± 1.3	35.3 ± 1.2
Male	5 (3)	214.1 ± 5.7	18.6 ± 1.6	30.1 ± 1.2	35.2 ± 0.7	35.3 ± 0.8
Female	21 (15)	223.0 ± 8.6	20.2 ± 1.6	30.9 ± 1.4	35.4 ± 1.7	35.4 ± 1.6
Unknown	62 (45)	220.5 ± 6.0	19.3 ± 1.4	30.4 ± 1.2	35.4 ± 1.2	35.4 ± 1.1
Class	Sample Size	50% Width	60% Width	70% Width	80% Width	90% Width
Calf	18 (8)	24.4 ± 0.9	19.4 ± 1.2	14.1 ± 1.3	8.6 ± 1.0	5.7 ± 0.8
Adult (All)	88 (63)	31.8 ± 1.5	25.2 ± 1.4	17.8 ± 1.4	10.3 ± 1.1	6.6 ± 1.0
Male	5 (3)	30.9 ± 1.1	26.1 ± 1.5	17.6 ± 2.4	10.4 ± 0.6	6.5 ± 0.5
Female	21 (15)	31.9 ± 1.8	25.3 ± 1.2	17.4 ± 1.1	10.4 ± 1.3	6.8 ± 1.1
Unknown	62 (45)	31.9 ± 1.4	25.2 ± 1.5	18.0 ± 1.4	10.3 ± 1.1	6.6 ± 1.1

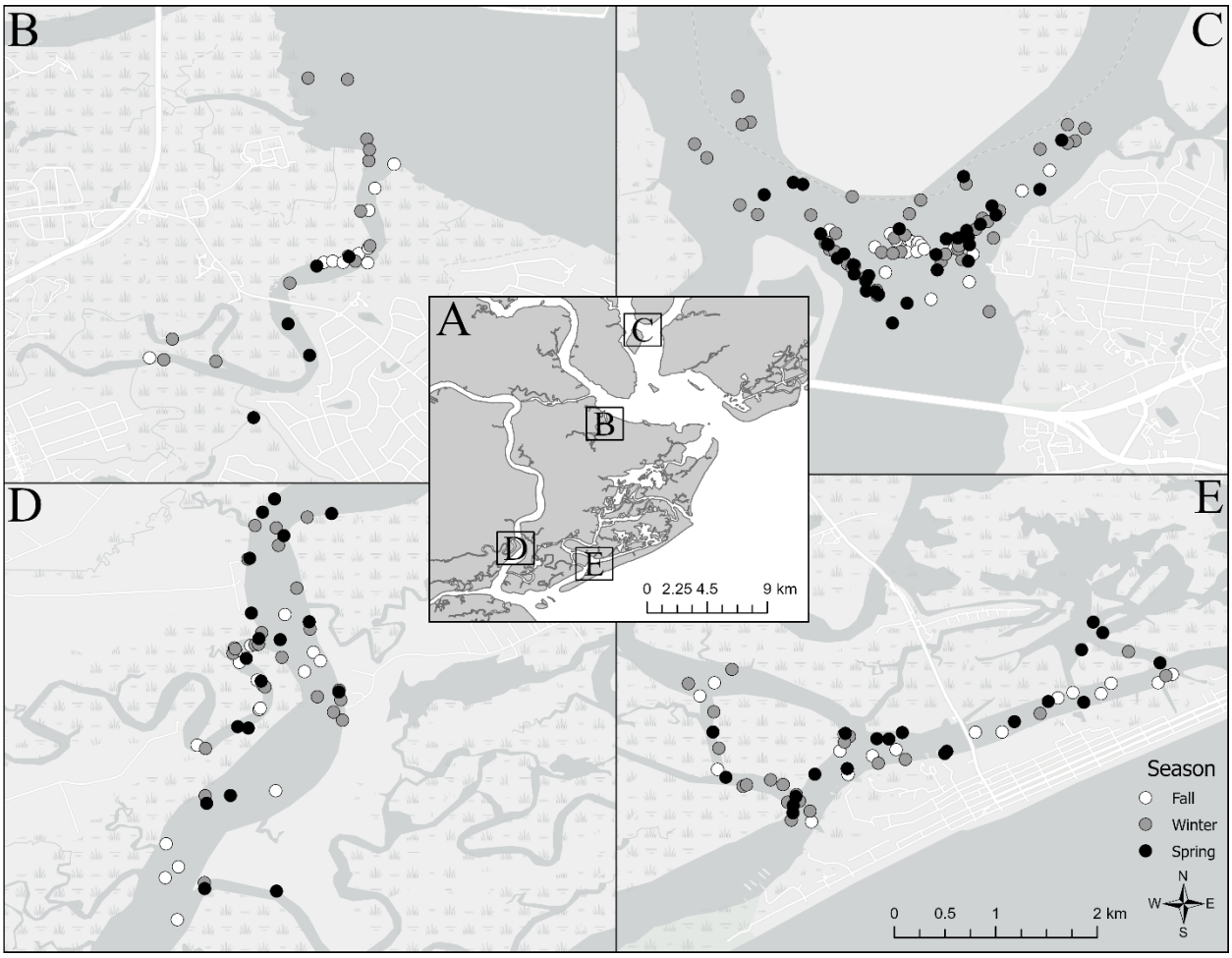

Figure 1. Locations of Tamanend's bottlenose dolphin (Tursiops erebennus) sightings (n = 239) at each of the four sites during land-based UAS flights in the Charleston Estuarine System (CES), South Carolina, during the fall (September to November), winter (December to February), and spring (March to May). (A) An overview of the CES, including the locations of the four study sites: (B) James Island Creek, (C) the Drum Island confluence area, (D) the Stono River Estuary, and (E) the Folly River.

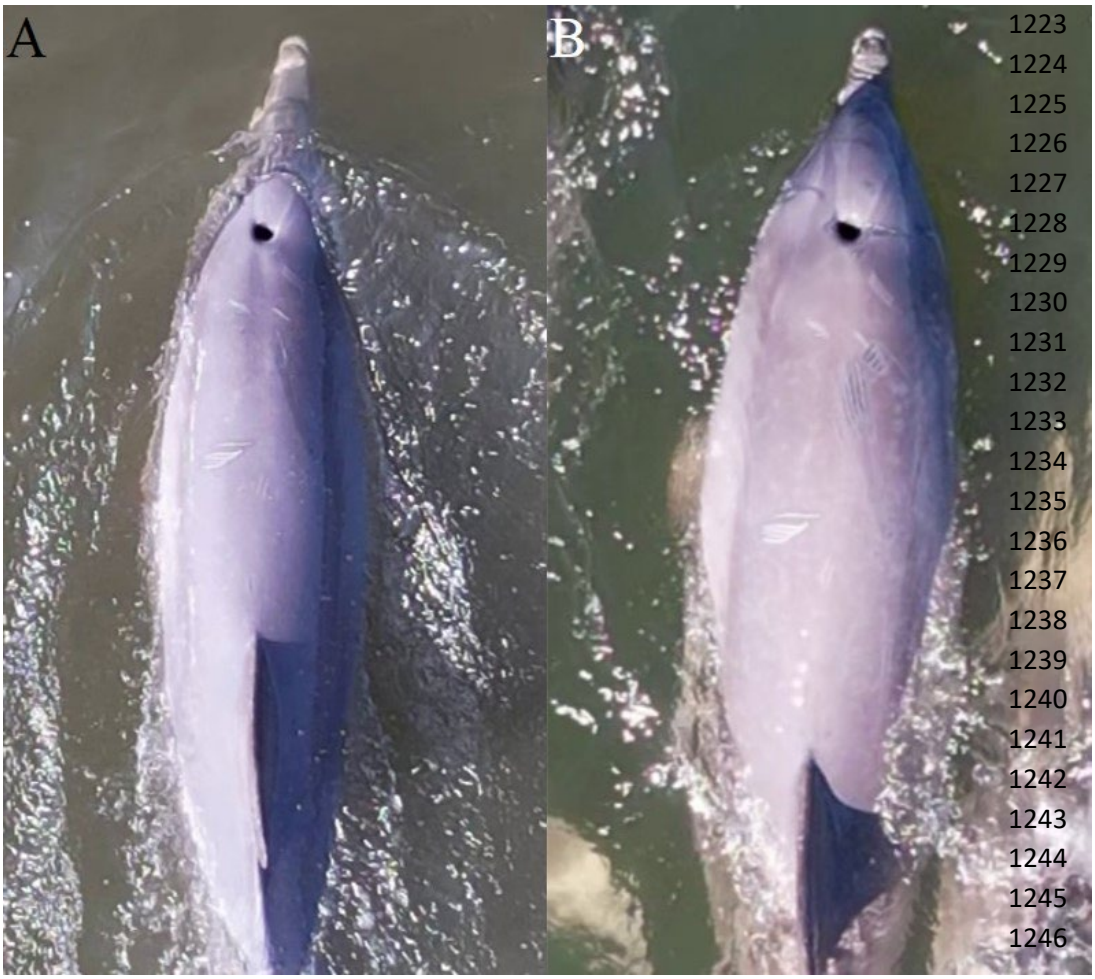

Figure 2. A Charleston Estuarine System Stock (CESS) dolphin that was identified during multiple UAS surveys based on its unique scars that were visible in UAS imagery. Matches were made by comparing each dolphin's distinct skin pigmentation and scarring patterns to individuals in the Drone Dolphin ID database. This dolphin (ID number 120) was observed during (A) Drum Island survey #24 on 25 February 2023 and (B) Drum Island survey #26 on 16 March 2023. (Both drone images taken by Colin M. Perkins-Taylor)

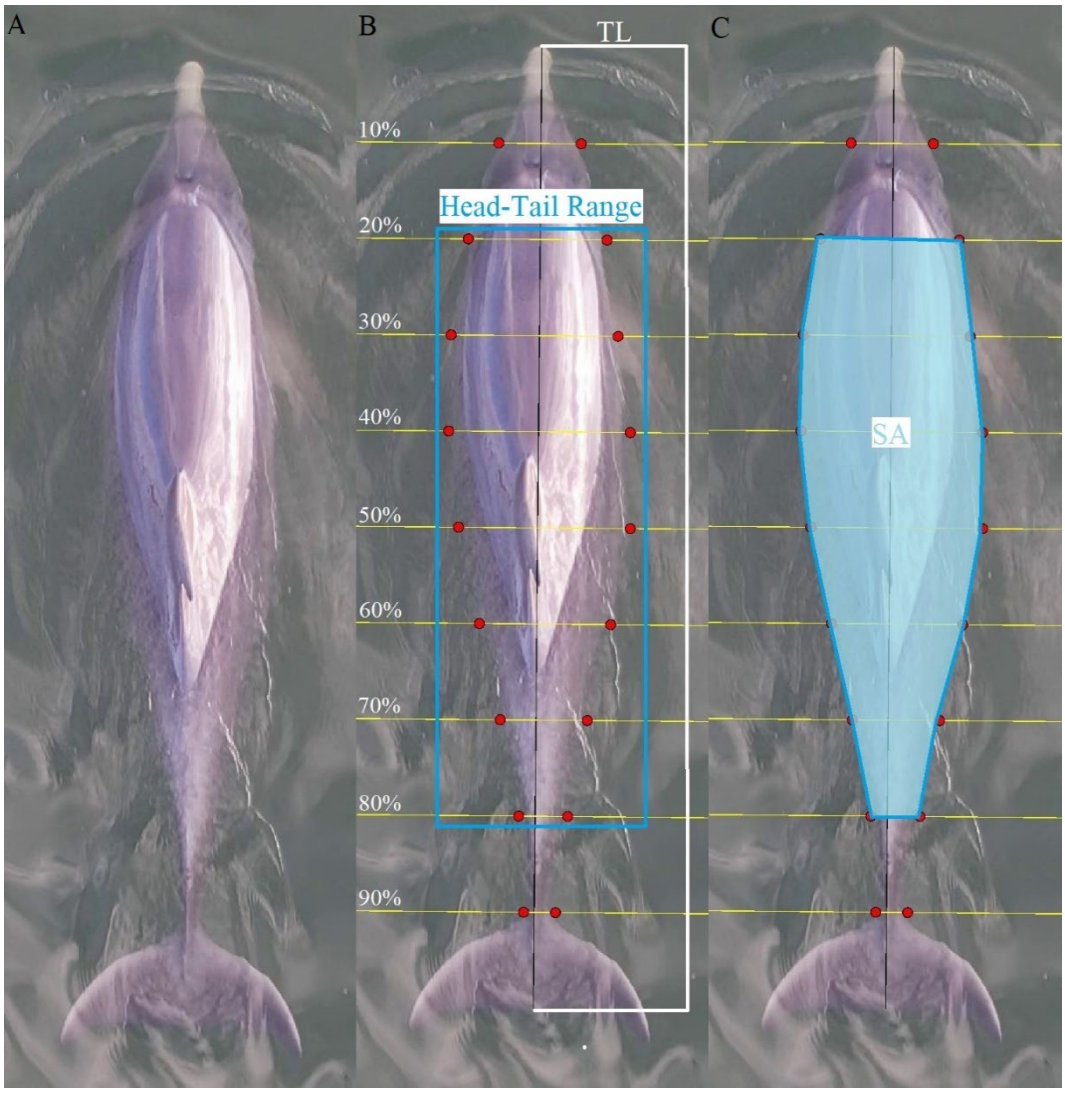

Figure 3. Example image of a Tamanend's bottlenose dolphin extracted from UAS video and the morphometric measurements calculated using photogrammetry following the methods described by Burnett et al. (2018): (A) extracted image of a dolphin while it was flat at the surface and its body shape was clearly distinguishable; (B) measurements calculated include total length (TL) and body widths at 10% intervals along the TL—the Head-Tail Range shows the region of the body included in the Body Area Index (BAI) calculation; and (C) body surface area (SA) of the dolphin based on parabolas, which is then used to calculate BAI. (All drone images taken by Colin M. Perkins-Taylor)

1284

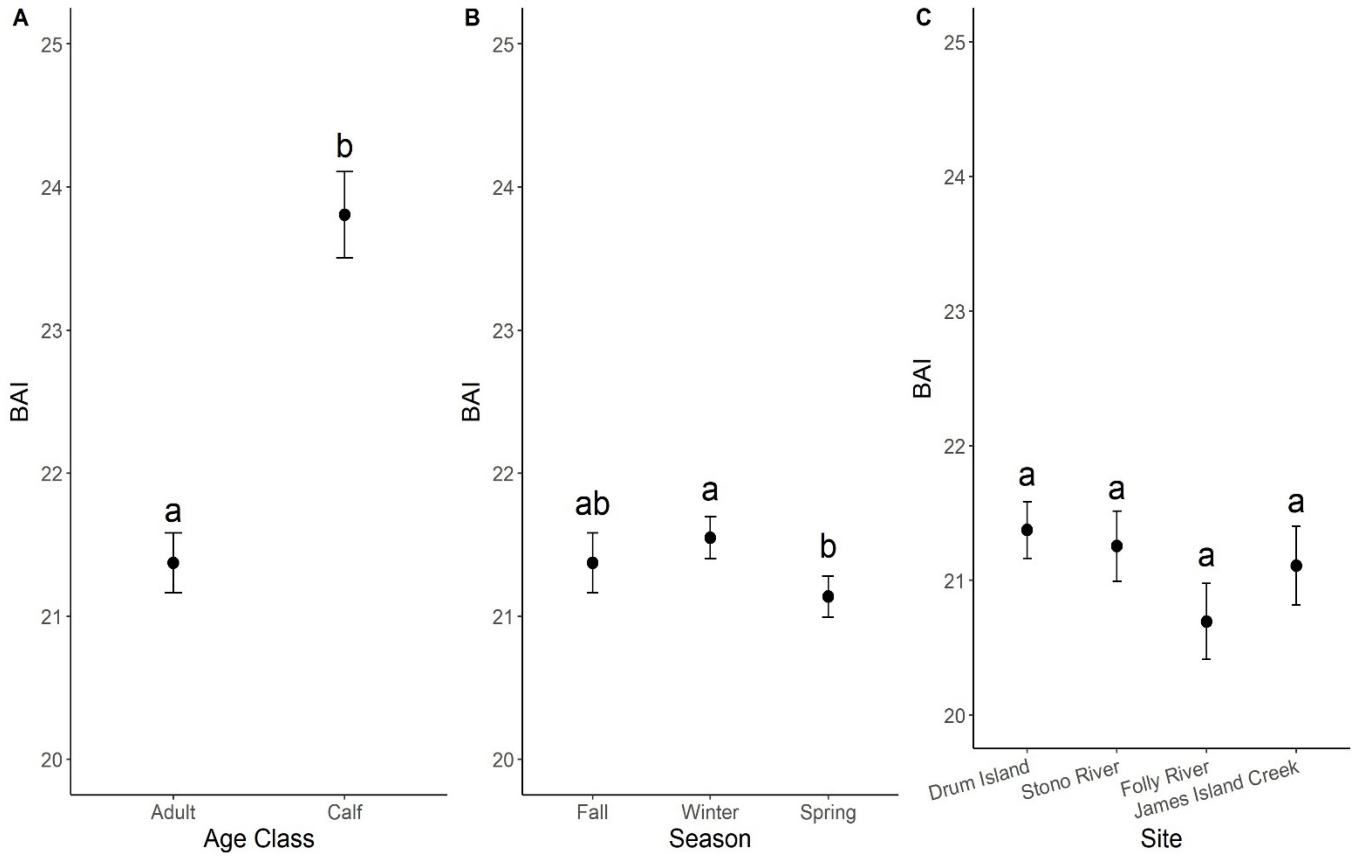

Figure 4. Body Area Index (BAI) of Tamanend's bottlenose dolphins in the CES between September 2022 and May 2023 based on different factors, including (A) age class, (B) season, and (C) site. Values were derived from the linear mixed effects model results with Dolphin ID (i.e., individual dolphin identity) as a random effect. Letters show groups that are significantly different from one another ($p < 0.05$) within each factor.

1285
1286
1287
1288
1289
1290
1291
1292
1293
1294
1295
1296
1297

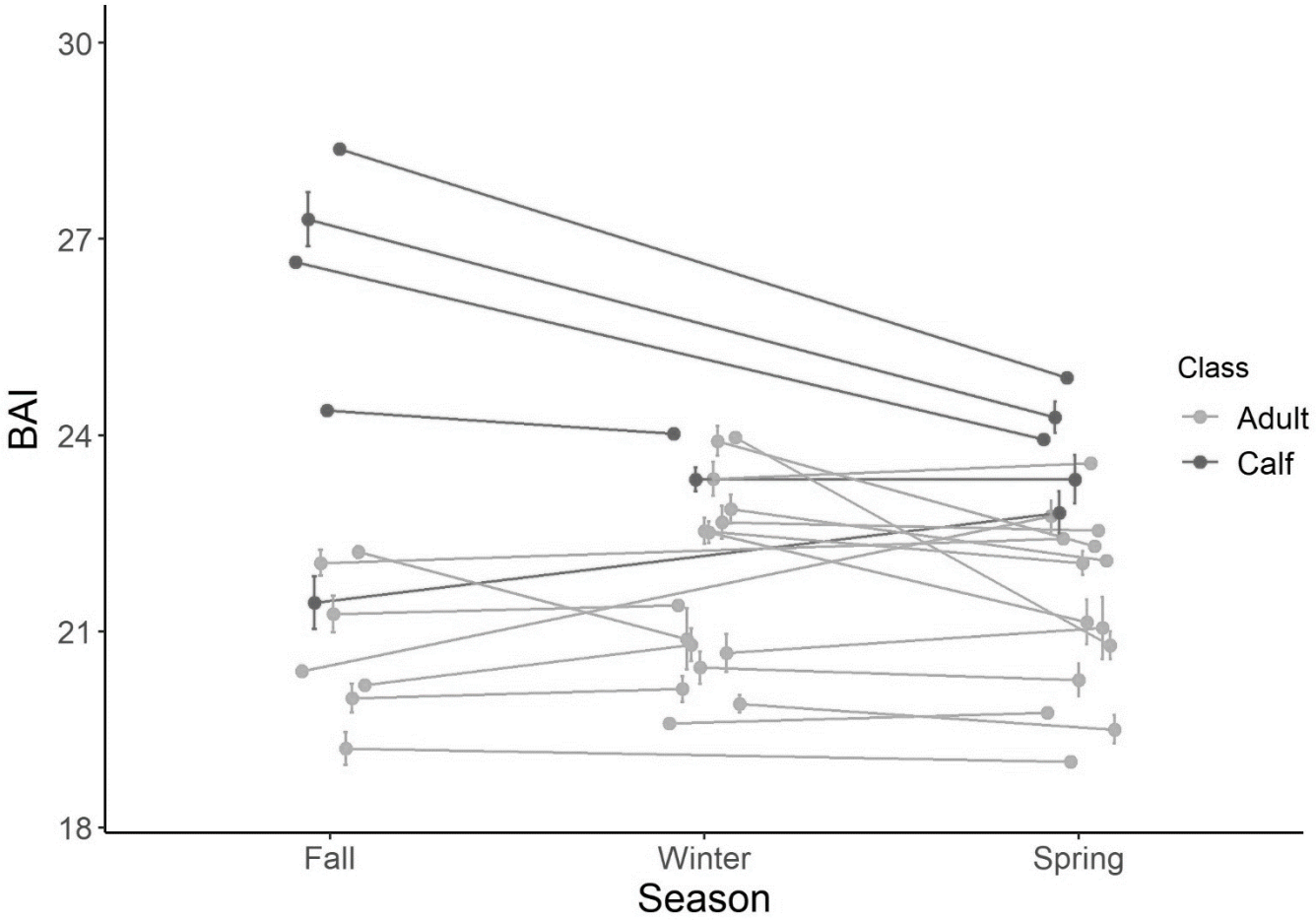

Figure 5. Seasonal body condition variation of Tamanend's bottlenose dolphins (n = 24) in the CES that had their Body Area Index (BAI) estimated during multiple seasons. Points with error bars (± SD) mean that multiple images of the individual from that season were included in the final analysis.

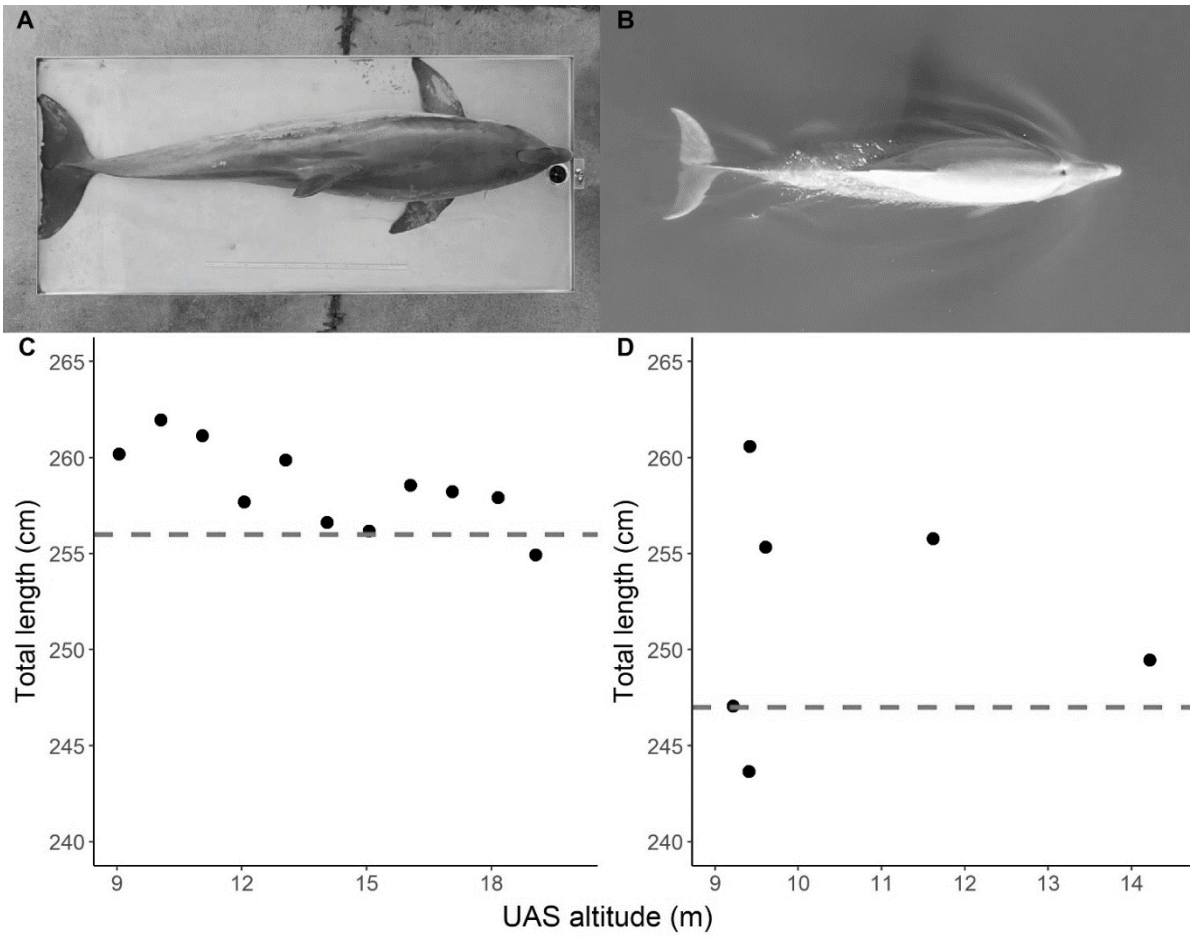

1312

Figure 6. Comparison of UAS total length (TL) estimates between (A) SC2303, a stranded male Tamanend's bottlenose dolphin, and (B) FB810, a known male CESS dolphin, with UAS TL estimates of (C) SC2303 and (D) FB810. The dashed line represents the measured TL of each individual. SC2303 was measured on its stranding date, while FB810 was measured during a live-capture health assessment in 1999, so his TL may have increased since then. (Drone images taken by Colin M. Perkins-Taylor)